The American Journal of Pathology, Vol. 169, No. 6, December 2006

DOI: 10.2353/ajpath.2006.051021

Gastrointestinal, Hepatobiliary and Pancreatic Pathology

Differential Angiogenic Regulation of Experimental Colitis

John H. Chidlow, Jr.,*† Will Langston,† James J.M. Greer,* Dmitry Ostanin,† Maisoun Abdelbaqi,* Jeffery Houghton,† Annamalai Senthilkumar,‡ Deepti Shukla,* Andrew P. Mazar,§ Matthew B. Grisham,† and Christopher G. Kevil*†

From the Departments of Pathology, Molecular and Cellular Physiology,† and Cardiology,‡ Louisiana State University Health Sciences Center–Shreveport, Shreveport, Louisiana; and Attenuon,§ San Diego, California*

Inflammatory bowel diseases (IBDs) are chronic inflammatory disorders of the intestinal tract with unknown multifactorial etiology that, among other things, result in alteration and dysfunction of the intestinal microvasculature. Clinical observations of increased colon microvascular density during IBD have been made. However, there have been no reports investigating the physiological or pathological importance of angiogenic stimulation during the development of intestinal inflammation. Here we report that the dextran sodium sulfate and $CD4^+CD45RB^{high}$ T-cell transfer models of colitis stimulate angiogenesis that results in increased blood vessel density concomitant with increased histopathology, suggesting that the neovasculature contributes to tissue damage during colitis. We also show that leukocyte infiltration is an obligatory requirement for the stimulation of angiogenesis. The angiogenic response during experimental colitis was differentially regulated in that the production of various angiogenic mediators was diverse between the two models with only a small group of molecules being similarly controlled. Importantly, treatment with the anti-angiogenic agent thalidomide or ATN-161 significantly reduced angiogenic activity and associated tissue histopathology during experimental colitis. Our findings identify a direct pathological link between angiogenesis and the development of experimental colitis, representing a novel therapeutic target for IBD. ***(Am J Pathol 2006, 169:2014–2030; DOI: 10.2353/ajpath.2006.051021)***

The inflammatory bowel diseases (IBDs), including Crohn's disease and ulcerative colitis, are chronic inflammatory disorders of the intestinal tract that are thought to arise from a complex interaction among the environment, the immune system, and genetics of affected individuals.[1–5] Although the specific causes of IBD are not well understood, several hallmark pathological features have been defined. The pathology of IBD invariably involves a chronic inflammatory cycle characterized by leukocyte infiltration, intestinal mucosa damage, ulceration, and regeneration. Recent clinical studies of active IBD have alluded to an increase in angiogenesis.[6,7] These studies suggest that stimulation of angiogenesis may play an important pathophysiological role in establishing and sustaining tissue inflammation, thereby playing an integral role in IBD pathology. Specifically, Spalinger and colleagues[6] have reported increased vessel density with Doppler ultrasonography during active Crohn's disease that is not enhanced in unaffected tissue or during disease remission. Moreover, a report by Fishman and colleagues[8] has demonstrated long-term remission of an individual with active Crohn's disease using the anti-angiogenic agent thalidomide. However, the pathological nature and importance of increased angiogenesis during IBD or experimental colitis is not known.

Angiogenic cytokine production has been reported to be elevated during IBD, possibly governing increased neovascularization during disease. Serum from IBD patients was reported to contain elevated concentrations of vascular endothelial growth factor (VEGF)-A during active disease versus remission.[9–11] A recent report by Konno and colleagues[12] has also shown elevated local tissue concentrations of VEGF-A in IBD specimens that may be more relevant in relation to IBD pathology, as it has been shown that local microenvironment tissue levels of VEGF-A are key in determining normal versus pathological angiogenesis.[12,13] Moreover, studies have also

Supported by the National Institutes of Health (grant DK 65649) and the Center for Excellence in Arthritis and Rheumatology at Louisiana State University Health Sciences Center–Shreveport.

Accepted for publication August 15, 2006.

Address reprint requests to Christopher G. Kevil, Ph.D., Department of Pathology, LSU Health Sciences Center–Shreveport, 1501 Kings Highway, Shreveport, LA 71130. E-mail: ckevil@lsuhsc.edu.

shown increases in serum levels of basic fibroblast growth factor (b-FGF) and transforming growth factor (TGF)-β in patients with active ulcerative colitis (UC) or Crohn's disease (CD).[10,14] Together, these reports clearly demonstrate that angiogenic cytokines are increased in patients with active IBD. However, no information is available regarding distinct expression profiles of pro- versus anti-angiogenic molecules during colitis.

Increased leukocyte infiltration is a hallmark feature of IBD and experimental colitis, with T cells, monocytes, and neutrophils contributing to disease initiation and subsequent tissue damage.[15–18] In addition to their role in the inflammatory response, leukocytes may also regulate angiogenic activity. Several studies have shown that various leukocyte types produce diverse angiogenic factors and can also modify extracellular matrix thereby promoting neovascularization.[19–21] Neutrophils have been reported to be significant sources of cytokines, such as interleukin (IL)-8 and VEGF, as well as matrix metalloproteinases (MMP-2 and -9) that are released at the site of inflammation to regulate angiogenesis.[22,23] Monocytes and macrophages also have corresponding roles in angiogenesis as sources of cytokines such as VEGF, FGFs, interferon-γ, tumor necrosis factor (TNF)-α, and many others.[24–26] It is widely accepted that T cells regulate IBD pathogenesis through the production of proinflammatory cytokines, such as Th1 cytokines, that are primarily proangiogenic concomitant with reduced production of regulatory cytokines, such as Th2 cytokines, that may have angiostatic or anti-angiogenic effects.[27–29] Therefore, infiltrated T cells could elicit diverse angiogenic regulation through the production of a wide array of angiogenic molecules including Th1 and Th2 cytokines and chemokines. Thus it is very likely that leukocyte infiltration with concomitant production of angiogenic mediators facilitates neovascularization and chronic inflammation observed in IBD.

Here we examine the hypothesis that increased angiogenic activity plays an important pathological role in two different models of experimental colitis. Data contained herein demonstrate that blood vessel density increases during colitis and strongly correlates with pathological scores of affected tissue. Moreover, we report that angiogenic stimulation in both models shows some similarities, as well as distinct differences, in angiogenic gene and protein profile expression, demonstrating a diverse angiogenic response. Data are also presented that demonstrate an essential requirement of leukocyte infiltration for angiogenic stimulation during colitis. Last, we report that anti-angiogenic intervention significantly attenuates leukocyte infiltration and tissue damage associated with experimental colitis, indicating that increased angiogenesis during colitis plays an important pathological role during disease. Together, these data provide compelling evidence for an important pathophysiological role of increased angiogenic activity during experimental colitis and highlight the potential for anti-angiogenic intervention as a novel therapeutic target for IBD.

Materials and Methods

Animals

Mice used for this study were bred and housed at the Association for Assessment and Accreditation of Laboratory Animal Care, international-accredited Louisiana State University Health Sciences Center–Shreveport animal resource facility and maintained according to the National Research Council's Guide for Care and Use of Laboratory Animals. CD18-null$^{-/-}$ (*Itgb2^{tm2Bay}*) C57BL/6J and wild-type C57BL/6J mice were bred in-house. Male Rag-1$^{-/-}$-null (*Rag1^{tm1Mom}*) C57BL/6J mice were obtained from Jackson Laboratories (Bar Harbor, ME).

3% Dextran Sodium Sulfate (DSS) and CD4$^+$CD45RB^{high} T-Cell Transfer Models of Experimental Colitis

The 3% DSS and CD4$^+$CD45RB^{high} T-cell transfer models of colitis were performed as previously reported.[16,30] Ten- to 12-week-old wild-type or CD18$^{-/-}$-null male C57BL/6J mice were administered 3% DSS (TDB Consultancy AB, Uppsala, Sweden) in their drinking water for 6 days. Control cohorts were given regular drinking water. Animals were monitored for symptoms of disease progression as previously reported and sacrificed on the 7th day for analysis of various parameters described below. The 3% DSS cyclic colitis model was performed with slight modifications as previously reported.[31] In brief, 3% DSS was administered for 5 days (on) and then switched to regular water for another 5 days (off). This cycle was repeated three times, and mice were sacrificed at the end of the third off cycle.

CD4$^+$CD45RB^{high} T-cell-dependent colitis was induced in male Rag-1-null mice between 10 and 12 weeks of age using CD4$^+$ T cells from the spleens of donor female C57/B6J mice as previously reported.[16,32] In brief, CD4$^+$ T cells were enriched using the MACS system from Miltenyi Biotech for negative selection by magnetic cell sorting. Cells were then labeled with anti-fluorescein isothiocyanate (FITC) microbeads, and unlabeled cells were separated on a depletion column (column type CS; Miltenyi Biotech, Auburn, CA). Enriched CD4$^+$ T cells were labeled with biotin-conjugated anti-CD4 monoclonal antibody followed with streptavidin-670 and phycoerythrin-conjugated anti-CD45RB monoclonal antibody (PharMingen, La Jolla, CA) and fractioned into CD4$^+$CD45RB^{high} and CD4$^+$CD45RB^{low} cell populations by two-color sorting on a FACS Vantage (Becton, Dickinson and Company, Mountain View, CA). The CD45RB^{high} population was defined as the brightest 40% and that of the CD45RB^{low} were the dimmest 15%. Next, 5×10^5 CD4$^+$CD45RB^{high} or CD4$^+$CD45RB^{low} cells were injected intraperitoneally in 500 μl of phosphate-buffered saline (PBS). Animals were monitored throughout 8 weeks for the development of experimental colitis and sacrificed at the end of week 8 for analysis of the various parameters described below.

Histopathological Scoring of Experimental Colitis

Pathological scoring of paraffin-embedded hematoxylin and eosin (H&E)-stained sections of the distal colons from DSS and $CD4^+CD45RB^{high}$ T-cell transfer experimental colitis mice was performed in a double-blinded manner. Histopathological scoring of DSS-treated colons was performed as previously reported.[30] In brief, these are severity of inflammation, scored 0 to 3 for none, slight, moderate, and severe; depth of injury, scored 0 to 3 for none, mucosal, mucosal, and submucosal, transmural; and crypt damage, scored 0 to 4 for none, basal one-third damaged, basal two-thirds damaged, only surface epithelium intact, entire crypt epithelium lost. Each sample received a score of 0 to 40 based on multiplying the score of each parameter by the percentage of tissue involvement (×1, 0 to 25%; ×2, 25 to 50%; ×3, 50 to 75%; ×4, 75 to 100%) and summing these values. Histopathological analysis of $CD4^+CD45RB^{high}$-induced colitis was performed as previously reported.[16] Eight parameters were used and included 1) the degree of inflammation in the lamina propria (range, 1 to 3); 2) goblet cell loss indicative of mucin depletion (range, 0 to 2); 3) reactive epithelial hyperplasia/atypia with nuclear changes (range, 0 to 3); 4) number of intraepithelial lymphocytes in the epithelial crypt (range, 0 to 3); 5) abnormal crypt architecture (range, 0 to 3); 6) number of crypt abscesses (range, 0 to 2); 7) mucosal erosion to frank ulceration (range, 0 to 2); and 8) submucosal spread to transmural involvement (range, 0 to 2). The severity of inflammatory changes is based on the sum of the scores in each parameter with a maximal score of 20.

Determination of Tissue Angiogenic Index

Distal colon segments from both models were frozen in OCT compound (Sakura Finetek USA, Inc., Torrance, CA). Ten-μm frozen cross-sections were fixed with 95% ethanol/5% glacial acetic acid for 20 minutes at −20°C, washed three times with PBS, blocked with 5% horse serum/PBS, and then stained with anti-mouse PECAM-1 (CD31) antibody (BD PharMingen) diluted 1:200 in PBS/0.05% horse serum followed by Cy3-conjugated anti-rat antibody diluted 1:250 in PBS with 0.05% horse serum. Slides were then mounted with Vectashield mounting medium containing 4,6-diamidino-2-phenylindole (DAPI) nuclear counterstain (Vector Laboratories, Inc., Burlingame, CA). Digital images were taken at a magnification of ×200 on a Nikon Eclipse TE2000-S epifluorescent scope (Melville, NY) using Texas Red and DAPI excitation/emission filters in conjunction with a Hamamatsu Orca-ER digital camera (Bridgewater, NJ). The total pixel density of PECAM-1 and DAPI staining was quantified for each image using Simple PCI software (C-Imaging Systems; Compix Inc., Sewickley, PA). All imaging settings for each respective fluorochrome were kept constant between specimens and the amount of PECAM-1 and DAPI pixel density measured using the image processing and analysis feature of Simple PCI. Total PECAM-1 pixel density was divided by the total DAPI pixel density for each image to calculate a vascular density ratio referred to as the angiogenic index.

Dual Radiolabel Antibody Measurement of Vascular Surface Area

A PECAM-1 dual radiolabel assay was used to quantify vascular surface area in the colons of DSS and $CD4^+CD45RB^{high}$ T-cell transfer experimental colitis mice. On completion of the experimental protocols, the animals were volume exchanged with radiolabeled PECAM-1 and control antibodies as previously reported.[33] Binding antibodies against PECAM-1 were labeled with ^{125}I (DuPont NEN, Boston, MA), and nonbinding control antibodies were labeled with ^{131}I (DuPont NEN) using the chloramine T method with resulting specific activities of 0.5 μCi/μg. Animals were anesthetized with xylazine/ketamine, and the carotid artery and jugular vein were cannulated and injected with the radiolabeled antibodies through the jugular vein with 0.2 ml of heparinized saline. After 4 minutes and 45 seconds, 250 μl of blood was obtained from the carotid line to determine end-point binding. The animal was then flushed with 6 ml of bicarbonate-buffer salt solution at pH 7.4 through the jugular to clear the thoracic organs. The inferior vena cava was then cut, and the animal was flushed with 15 ml of bicarbonate-buffer salt solution through the carotid to clear the abdominal organs. Organs were then harvested and weighed, and the activity of ^{125}I and ^{131}I in the colons was measured using a 14800 Wizard 3 gamma counter (Wallac Instruments, Wellesley, MA) with automatic correction for background activity and spillover. The total injected activity in each experiment was calculated by counting a 2-μl sample of the radiolabeled monoclonal antibody (mAb) mixture. The radioactivities remaining in the tube used to mix the mAbs and the syringe used to inject the mixture were subtracted from the total injected activity. PECAM-1 antibody binding was calculated by subtracting the accumulated activity per gram of tissue of the nonbinding mAb from the activity of the binding mAb and expressed as micrograms of mAb per gram of tissue using the following equation: (μg mAb/g) = {[%ID[^{125}I/g tissue] − %ID[^{131}I/g tissue] × %ID(^{125}I)plasma/%ID(^{131}I)plasma} × total binding mAb (μg)/100, where ID represents injected dose.

FITC-Labeled Lycopersicon esculentum Lectin Labeling of Colon Vasculature

FITC-labeled *L. esculentum* lectin (Vector Laboratories) labeling was used to independently validate the PECAM-1 staining technique and to evaluate if the neovasculature was perfused. Lectin labeling of the vasculature in distal colons of DSS and $CD4^+CD45RB^{high}$ T-cell transfer colitis models was performed as previously reported.[34] On completion of the colitis protocols, mice were anesthetized, and the inferior vena cava was cannulated. One hundred μg of the lectin in 100 μl of 0.9%

NaCl was perfused into the tail vein. The lectin was allowed to circulate for 2 minutes before fixative, 0.5% glutaraldehyde and 1% paraformaldehyde in PBS, was perfused through the vena cava. Eight-μm frozen cross-sections were made using the same tissue processing method described for PECAM-1 staining. The slides were then mounted in DAPI Vectashield mounting medium (Vector Laboratories) and analyzed for FITC-lectin pixel density to determine a lectin angiogenic index. Additional sections were also stained for PECAM-1 and three-color images acquired (PECAM-1, lectin, and DAPI).

Angiogenesis Gene Array

Mouse Angiogenesis Gene Array kits from SuperArray Biosciences Corp., Frederick, MD, were used to assay levels of angiogenic gene expression in experimental colitis. Total RNA was isolated from colon tissue of DSS and $CD4^+CD45RB^{high}$ colitic and control mice as previously reported.[16,35] Colon samples were snap-frozen in liquid nitrogen and then ground with a mortar and pestle kept cold on liquid nitrogen. Samples were then placed in Dounce homogenizers containing 600 μl of buffer RLT as specified by Qiagen's RNeasy protocol (Qiagen, Valencia, CA). RNA isolation was performed according to the manufacturer's protocol. RNA concentration and purity were measured by UV absorbance at 260 nm and 280 nm.

Gene array membranes were prehybridized using the GEAhyb hybridization solution containing sheared salmon sperm DNA and incubated at 60°C for 2 hours using a VWR Scientific Products (West Chester, PA) hybridization oven. Probe synthesis was done according to the GE Array Ampo Labeling-LPR kit protocol using total RNA from colon tissue. After prehybridization, the labeled cDNA probes were denatured and added to the arrays. Gene arrays were hybridized overnight at 60°C at 10 rotations per minute. Arrays were then washed three times in 1× standard saline citrate and washed again three times in 0.1× standard saline citrate. The arrays were then blocked for 1 hour in blocking buffer and incubated with alkaline phosphatase for 1 hour in 1× buffer F (SuperArray). The arrays were then washed and incubated in CPD star for 5 minutes and exposed to Blue Bio film (Denville Scientific, Inc., Metuchen, NJ) and developed using a Konica SRX-101 film developer (Konica Inc., Ramsey, NJ).

VEGF-A Western Blotting and Serum and Tissue Enzyme-Linked Immunosorbent Assays (ELISAs)

VEGF-A Western blot and ELISA were performed as previously reported.[36,37] Serum was obtained from controls, DSS-treated, and $CD4^+CD45RB^{high}$-treated mice as follows. A retro-orbital bleed was used to collect ~1 ml of blood from all mice at the time of death. These samples were kept on ice for 30 minutes and then spun at 3000 rpm for 10 minutes to obtain serum. Serum was collected in 50-μl aliquots and stored at −80°C. Tissue lysates were made from 15- to 20-mm segments of distal colon tissue from controls, DSS, and $CD4^+CD45RB^{high}$ colitic mice as follows. Samples were snap-frozen in liquid nitrogen and later homogenized in 500 μl of radioimmunoprecipitation assay lysis buffer containing protease inhibitors. The homogenized tissue was placed in a 1.5-ml microcentrifuge tube and spun for 30 minutes at 12,000 rpm at 4°C. The supernatant was removed and placed in a clean microcentrifuge tube and spun down two more times to obtain a clear lysate. The samples were aliquoted, and the protein concentration determined using the Bio-Rad DC protein assay kit (Bio-Rad, Hercules, CA).

VEGF-A Western blot analysis was performed as previously reported.[36,37] In brief, 50 μg of total protein from each sample was separated using 10% sodium dodecyl sulfate-polyacrylamide gel electrophoresis at 150 V. Proteins were transferred to Immuno-Blot polyvinylidene difluoride membrane (Bio-Rad) and subsequently blocked for 6 hours at 4°C in 5% milk TBS-T. Polyclonal anti-murine VEGF-A_{164} antibody (Peprotech, Inc., Rocky Hill, NJ) was applied at a concentration of 2 μg/ml and incubated overnight at 4°C. Anti-rabbit IgG-horseradish peroxidase-linked secondary antibody (Amersham Biosciences, Arlington Heights, IL) was applied at a 1:2000 dilution and incubated for 3 hours at room temperature in 5% milk TBS-T. The membrane was then incubated in ECL Western blotting detection reagents (Amersham Biosciences) for 10 minutes, exposed to Blue Bio film (Denville Scientific, Inc.), and developed using a Konica SRX-101 film developer (Konica, Inc.).

Quantitative measurement of VEGF-A levels was performed using a mouse VEGF-A ELISA kit according to the manufacturer's protocol (Oncogene, Boston, MA). In brief, 50 μl of assay diluent RD1N was pipetted into each well along with 50 μl of the samples and mixed by shaking the plate for 1 minute. The plate was then sealed and incubated at room temperature for 2 hours. Wells were washed five times with 1× wash buffer, and 100 μl of 1× mouse VEGF conjugate concentrate was then added to each well. The plate was again sealed and incubated for 2 hours. Wells were washed five times, and 100 μl of substrate solution was then added and incubated for 30 minutes. The reaction was terminated using 100 μl of stop solution and then read on a TECAN GENios Plus multiscan plate reader (Phenix Research Products, Candler, NC) at dual wavelengths of 450/540 nm.

Use of Anti-Angiogenic Agents during Experimental Colitis

Ten- to 12-week-old wild-type C57BL/6J mice undergoing DSS-induced colitis were treated with the anti-angiogenic agent thalidomide (Calbiochem, La Jolla, CA). Thalidomide (200 mg/kg) in dimethyl sulfoxide was administered intraperitoneally on days 0, 2, 4, and 6 of the model. Control animals were injected with an equal amount of dimethyl sulfoxide alone at the same time points. Colon tissue was harvested and processed for

H&E pathological scoring and angiogenic index determination as described above.

ATN-161 (Ac-PHSCN-NH2), a 5-mer peptide that binds to $\alpha_5\beta_1$ and $\alpha_V\beta_3$, was used in the $CD4^+CD45RB^{high}$ colitis model to evaluate the effects of target-specific anti-angiogenic intervention.[38] Two weeks after $CD4^+CD45RB^{high}$ reconstitution of Rag-1-deficient mice, 1 mg/kg ATN-161 (active peptide) or ATN-163 (scrambled peptide) in PBS was administered by intraperitoneal injection three times a week for the remaining 6 weeks of the study protocol. On completion of week 8, animals were sacrificed, and tissue was processed for various parameters described above.

Leukocyte Adhesion Under Hydrodynamic Flow Conditions

Hydrodynamic parallel plate flow chamber studies were performed as we have previously reported.[39] In brief, freshly isolated mouse splenocytes were labeled with a fluorescent dye by 30-minute incubation at 37°C with 200 nmol/L Cell Tracker Green purchased from Molecular Probes, Eugene, OR. The labeled cells were resuspended in Hanks' balanced salt solution at 2×10^5 cells/ml in a 200-ml beaker kept at 37°C and stirred at 60 revolutions per minute. A Glycotech flow chamber insert and gasket were used to form a laminar plate flow chamber that could be viewed on a microscope. Labeled splenocytes mixed with or without ATN-161 (10 μg/ml) were drawn from the beaker into the flow chamber across a monolayer of either unstimulated or TNF-α (10 ng/ml)-stimulated murine endothelial cells at a physiological shear rate of 1.5 dynes/cm^2 using a programmable digital syringe pump. The fluorescent cells were visualized using a Nikon Eclipse TE-2000 epifluorescent microscope equipped with a Hamamatsu digital camera, and digital video was captured at 29 images/second using SIMPLE PCI software from Compix. Firmly adherent cells were counted and defined as cells that did not move one cell diameter throughout a 5-second period as determined by automated tracking and manual review of individual cells in each experimental field of view.

Statistical Analysis

Control versus colitis data were compared against one another for each model of colitis. Statistical analysis of the data were determined using a Student's *t*-test with a value of $P < 0.05$ required to achieve significance. Temporal comparisons were performed by one-way analysis of variance with Dunnett's posttest. A value of $P < 0.05$ was required to achieve significance. *n* values for each experiment are reported in the figures. Data are reported as mean ± SE.

Results

Pathological Features of Experimental Colitis

Several different models of experimental colitis have been reported that display various pathophysiological aspects of IBD disorders including CD and UC.[15,40] Although no model serves as a complete surrogate for human disease, many salient clinical features can be examined depending on the agent or method used to induce experimental colitis. In this study, we used the DSS and $CD4^+CD45RB^{high}$ T-cell transfer models of colitis, which manifest similar disease characteristics of UC and CD. DSS induces colitis primarily by irritation and denudation of surface epithelium that quickly results in weight loss, loose stool/diarrhea, and occult and gross rectal bleeding.[41,42] We analyzed vehicle control and DSS-treated distal colons of C57/B6J mice. Prominent mucosal and submucosal leukocyte infiltrates were observed in 3% DSS-treated colons along with severe erosion of the epithelial cell layer often resulting in ulceration, significant mucosal/crypt damage, and submucosal edema. Lesions were intermittently located within the colon with the majority of histopathological changes observed in the distal segment (data not shown). $CD4^+CD45RB^{high}$ T-cell-induced colitis results from differential expansion of Th1 cells in Rag-$1^{-/-}$ mice, driven by enteric bacteria.[43,44] Similar, but less severe, leukocyte infiltration was observed in the $CD4^+CD45RB^{high}$ T-cell transfer model along with moderate erosion of the epithelial cell layer and mucosal/crypt damage compared with $CD4^+CD45RB^{low}$ control colons that do not develop disease (data not shown). Blinded analysis of the histopathology was done, and the scoring of pathological changes showed a significant increase in histopathological scores in both models, these being 23- and 17-fold in the DSS and $CD4^+CD45RB^{high}$ models, respectively, with the DSS model displaying greater disease severity. Together, these models display several important inflammatory pathophysiological features of human IBD.

Measurement of Blood Vessel Density in Experimental Colitis

Several clinical reports of IBD have observed an increase in colon vascular density during active disease.[6,7] However, no studies have examined the vascular density of actively inflamed colons from experimental models of colitis. Therefore, we used the well-established technique of anti-PECAM-1 (CD31) immunohistochemistry to measure changes in vascular density between the two colitis models.[45–48] Figure 1, A and B, illustrates the amount of PECAM-1 staining (red) in control and DSS-treated distal colons, respectively. Figure 1, C and D, shows secondary antibody control and DAPI alone staining of DSS-treated colons, respectively. Likewise, Figure 1, E and F, illustrates the amount of PECAM-1 staining in control $CD4^+CD45RB^{low}$ colons and $CD4^+CD45RB^{high}$ colons, respectively. Figure 1, G and H, demonstrates secondary

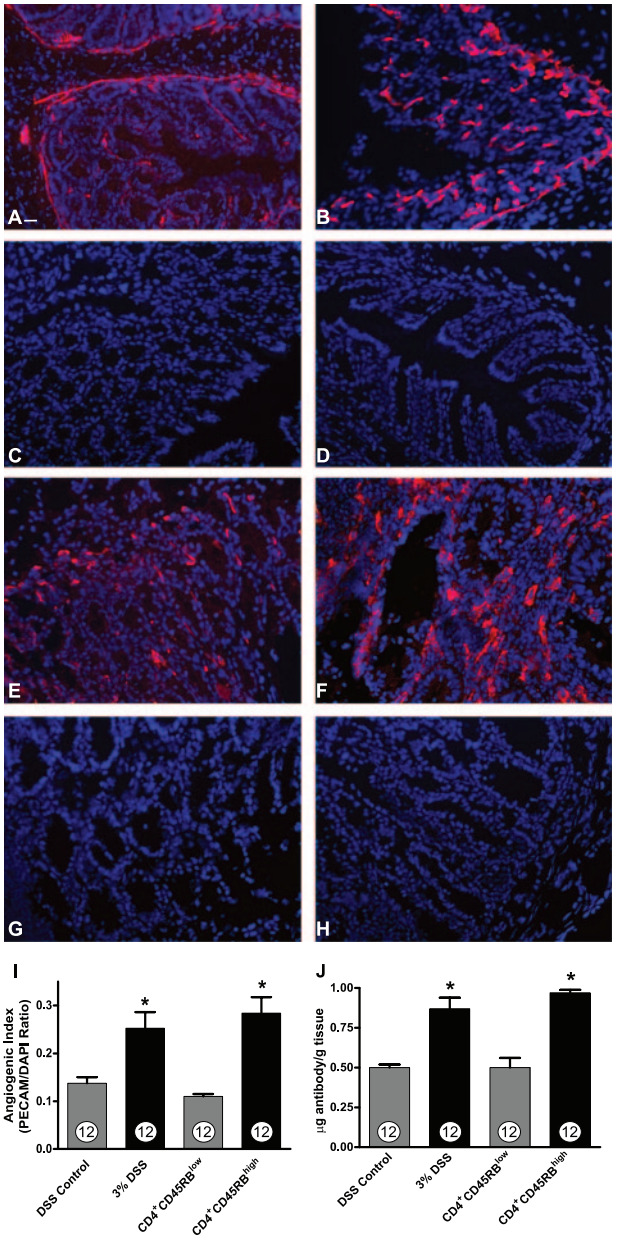

Figure 1. PECAM-1 blood vessel density measurement during experimental colitis. Vascular density of normal and diseased colons was determined by staining frozen sections with anti-PECAM-1 antibody (red) followed by DAPI nuclear counterstaining (blue). **A:** PECAM-1 staining of normal DSS vehicle-treated colon tissue. **B:** Increased PECAM-1 staining of 3% DSS-treated colon tissue. **C:** Secondary antibody control staining of DSS-treated colon tissue. **D:** DAPI alone staining of DSS-treated colon tissue. **E:** PECAM-1 staining of $CD4^+CD45RB^{low}$ T-cell transfer control colon tissue. **F:** Enhanced PECAM-1 staining of $CD4^+CD45RB^{high}$ T-cell transfer colitis tissue. **G:** Secondary antibody control staining of $CD4^+CD45RB^{high}$ T-cell transfer colitis tissue. **H:** DAPI alone staining of $CD4^+CD45RB^{high}$ T-cell transfer colitis tissue. **I:** Quantitative measurement of vascular density in the tissue sections as determined by calculating and angiogenic index that is derived from the total PECAM-1 surface area divided by the total DAPI surface area. **J:** The amount of radiolabeled PECAM-1 antibody binding within the colon vasculature demonstrating a significant increase in vessel surface area during experimental colitis. *n* values for each condition are reported within the bar graph. $^*P < 0.05$ versus control. Original magnifications, ×200. Scale bar = 100 μm.

antibody control and DAPI alone staining of $CD4^+CD45RB^{high}$ distal colons, respectively. To determine differences in vessel density, quantitative measurements of total PECAM-1 pixel surface area were made in conjunction with total surface area measurement of DAPI nuclear staining (blue) to calculate an angiogenic index. Figure 1I illustrates that both the DSS and $CD4^+CD45RB^{high}$ colitis models show a significant increase in the angiogenic index compared with respective controls. The PECAM-1 angiogenic index showed significant increases in vascular density in both models with the $CD4^+CD45RB^{high}$ model displaying a 188 ± 2.1% increase in vascular density and the DSS model an 89.7 ± 1.9% increase in vascular density. We further validated these observations by performing dual radiolabel experiments using ^{125}I-labeled anti-PECAM-1 to quantitatively measure the colon vascular surface area.[33,49] Figure 1J demonstrates increased anti-PECAM-1 antibody binding in both models of experimental colitis, confirming an increase in vascular density. Moreover, anti-PECAM-1 radiolabel data show a similar increase in blood vessel surface area compared with PECAM-1 immunofluorescent measurement of the angiogenic index. These data clearly demonstrate that experimental colitis results in a significant increase in colon vascular density.

Although PECAM-1 staining is a widely used method to quantitate vascular density, its expression has been observed on other cell types, albeit to a lesser extent, and the level of expression does not significantly fluctuate on inflammatory activation.[33,50–53] Nonetheless, we sought to independently verify the PECAM-1 angiogenic index data using FITC-labeled *L. esculentum* lectin to label the vasculature. *L. esculentum* lectin avidly binds vascular endothelium in a highly selective manner and has been previously used to determine angiogenic activity and vascular density.[54] Intravenous injection of FITC lectin was performed on control and experimental colitic mice to obtain a lectin angiogenic index. Colon tissue sections were also stained for PECAM-1 to evaluate co-localization in the same specimen. Figure 2A shows PECAM-1 staining of DSS distal colon, whereas Figure 2B illustrates the FITC lectin binding of the same section. Figure 2C shows the three-color merged image of lectin (green), PECAM-1 (red), and DAPI nuclear stain (blue). The majority of lectin and PECAM-1 staining co-localized throughout the tissue, with few areas showing distinct PECAM-1 staining alone. Figure 2D reports the FITC-lectin angiogenic index in both the DSS and $CD4^+CD45RB^{high}$ models compared with controls. The FITC-lectin angiogenic index corroborates the PECAM-1 angiogenic index for determining vascular density, with the lectin angiogenic index showing a 153 ± 1.4% increase in blood vessel density for the $CD4^+CD45RB^{high}$ model and 95 ± 1.3% in the DSS model. Moreover, the high degree of co-localization between lectin and PECAM-1 indicates perfusion of these vessels.

Increased Vascular Density Is Temporally Linked with Pathological Severity

Several chronic disease conditions have been associated with increased angiogenic activity.[55–57] Given the cyclical nature of IBD activity and remission, increased

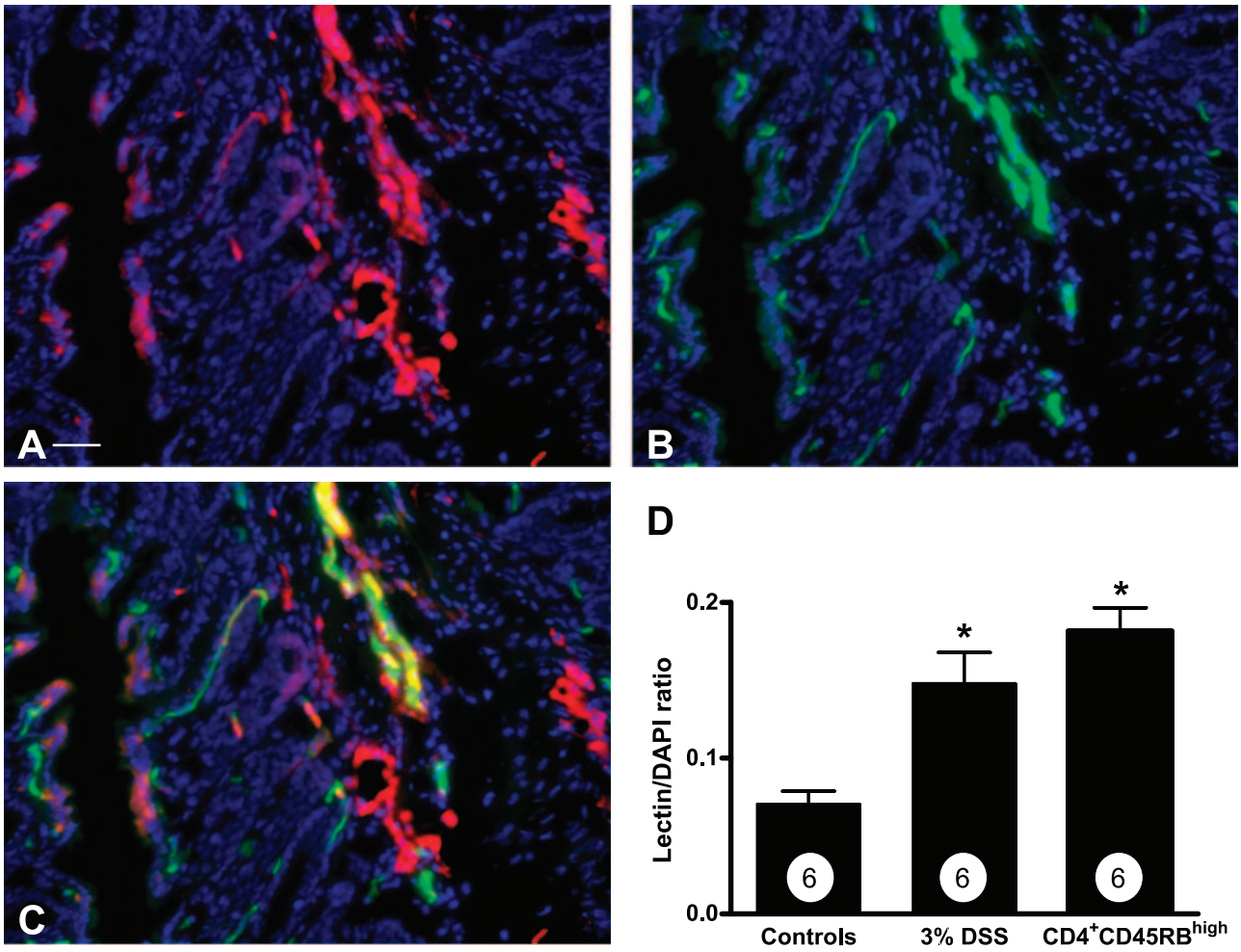

Figure 2. FITC *L. esculentum* lectin analysis of angiogenesis during experimental colitis. Fluorescently labeled *L. esculentum* lectin was injected intravenously to specifically stain endothelial cells to independently validate PECAM-1 antibody data as well as evaluate the perfusion of colitis-induced neovascularization. Distal colon tissue was also stained with PECAM-1 antibody to determine whether these markers of neovascularization co-localized with one another. **A:** PECAM-1 staining (red) of DSS-induced angiogenesis; **B:** FITC *L. esculentum* lectin intravascular labeling (green) of the same section. Importantly, **C** demonstrates a large amount of PECAM-1/lectin co-localization throughout the section. **D:** Lectin angiogenic index, which was obtained by dividing the total lectin surface area by the total DAPI surface area. *n* values for each condition are reported within the bar graph. $^*P < 0.05$ versus control. Original magnifications, ×200. Scale bar = 100 μm.

angiogenic activity may serve to facilitate tissue repair. However, no clear information exists regarding the relationship between angiogenic activity and disease severity in IBD or other chronic inflammatory disorders. Therefore, we examined the association of increased angiogenic activity with disease severity in specimens from both experimental colitis models. Ten-μm serial sections of distal colons were processed for H&E histopathology or anti-PECAM-1 angiogenic index to compare these parameters within the same tissue specimen. Figure 3, A and B, shows the correlation between angiogenic index and histopathology score for the DSS and $CD4^+CD45RB^{high}$ colitis models, respectively. Measurements made from identical specimens from either model show a strong and significant correlation between the angiogenic index and tissue histopathology score with the DSS model having an r^2 of 0.90 and the $CD4^+CD45RB^{high}$ model an r^2 of 0.91. Moreover, we also examined the temporal relationship between increased angiogenic activity and tissue histopathology in the DSS colitis model. Figure 3C illustrates that DSS-mediated angiogenic activity becomes significantly elevated at 4 days, which is precisely when significant tissue histopathology is observed (Figure 3D). We also examined angiogenic activity and tissue pathology on completion of a cyclical DSS regimen, in which 3% DSS is administered for 5 days and then withdrawn for 5 days (and switched to regular water), with this cycle being repeated three times. Cycling of the DSS treatment results in acute inflammatory periods followed by tissue restitution and repair, which may emulate cyclical aspects of human IBD.[31] Tissues were harvested at the end of the last off cycle that revealed histopathological changes, albeit greatly reduced, but that angiogenic activity was not significantly different from control (Figure 3D). These results combined with data from the acute DSS model indicate that increased angiogenic activity is associated with active inflammation and diminished during restitution. Together, these data strongly suggest that increased angiogenic activity

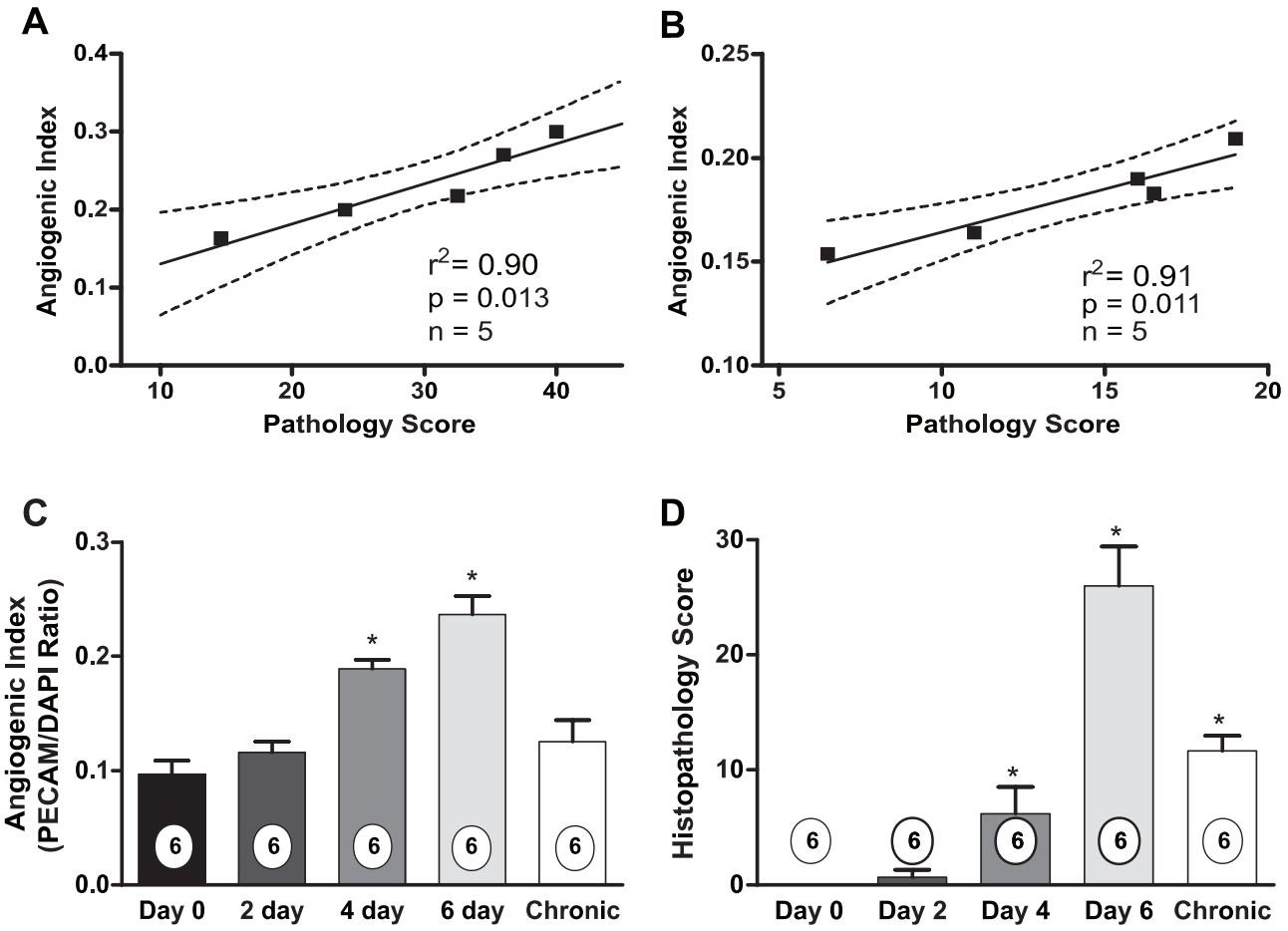

Figure 3. Relationships between angiogenic index and tissue pathology during experimental colitis. Serial tissue sections were obtained from both experimental colitis models to evaluate histopathological score and angiogenic index from identical specimens. Angiogenic index and pathological score data were plotted against one another and correlation indexes determined. **A:** Angiogenic index and tissue pathology scores closely correlate in the 3% DSS colitis model with an $r^2 = 0.90$. **B:** Angiogenic index and tissue pathology closely correlate in the $CD4^+CD45RB^{high}$ T-cell colitis model with an $r^2 = 0.91$. *P* values and *n* values for correlation determination are reported in each graph. **C:** Temporal nature of increased angiogenesis during DSS-mediated colitis. **D:** The temporal nature of tissue histopathology during DSS-mediated colitis. *n* values for each condition are reported within the bar graph. $^*P < 0.05$ versus day 0.

contributes to tissue histopathology during active experimental colitis.

Differential Regulation of Angiogenic Mediators during Experimental Colitis

It is now well accepted that the presence of high levels of proangiogenic factors play key roles in the process of pathological neovascularization as shown by studies that inhibit them.[58–60] Therefore, we examined expression profiles of angiogenic regulatory genes to gain a better understanding of the factors that may be involved in controlling angiogenesis during experimental colitis. Angiogenesis gene arrays were performed using total RNA isolated from four different control and DSS-treated colons on completion of a 6-day study and from four different $CD4^+CD45RB^{low}$ control or $CD4^+CD45RB^{high}$ experimental colons on completion of the 8-week study. Differentially regulated genes were identified based on a twofold change in signal intensity (up or down) compared with control signals. A complete list of the genes that were similarly or differentially regulated in the DSS and $CD4^+CD45RB^{high}$ colons as compared with their respective controls is shown in Table 1.

Similarly up-regulated proangiogenic mediators include matrix metalloproteinases 2 and 9 (MMP-2, -9), endothelial sphingolipid G-protein coupled receptor 1 (Edg1), endoglin, prostaglandin-endoperoxide synthase 2 (COX2), TNF-α, chemokine (CXC) ligand 1 (Gro1), and hepatocyte growth factor (HGF). Additional mediators that can exert either pro- or anti-angiogenic effects, depending on stimulation, were also similarly up-regulated in both models including TGF-βR2 and TGF-βR3, macrophage scavenger receptor 1 (Msr1), and thrombospondin-1 (Thbs 1). Three genes were also similarly down-regulated including CD36 antigen and chromogranin A, which are anti-angiogenic, and TGF-β2, which may act in either capacity. Of the similarly regulated genes, most up-regulated genes exhibit proangiogenic effects and most down-regulated ones exhibit anti-angiogenic effects. This suggests that the inflammatory stimulus involved with either model of experimental colitis elicits a proangiogenic response consistent with underlying pathological features between the two models.

Table 1. Angiogenesis Gene Expression Profiles in the 3% DSS and $CD4^{+}CD45RB^{high}$ T-Cell Colitis Models

3% Dextran Sodium Sulfate Colitis		$CD4^{+}CD45RB^{high}$ Colitis	
UP	**DOWN**	**UP**	**DOWN**
Matrix Metalloproteinase 2 (MMP2)	CD36 Antigen (CD36, Thrombospondin Receptor)	Matrix Metalloproteinase 2 (MMP2)	CD36 Antigen (CD36, Thrombospondin Receptor)
Matrix Metalloproteinase 9 (MMP9)	Chromogranin A (Chga)	Matrix Metalloproteinase 9 (MMP9)	Chromogranin A (Chga)
Endothelial Sphingolipid G-protein coupled receptor 1 (Edg1)	Transforming Growth Factor beta 2 (TGF-b2)	Endothelial Sphingolipid G-protein coupled receptor 1 (Edg1)	Transforming Growth Factor beta 2 (TGFb2)
Endoglin (Eng)	Vascular Endothelial Growth Factor A (VEGF-A)	Endoglin (Eng)	
Prostaglandin-endoperoxide synthase 2 (COX2)	Vascular Endothelial Growth Factor B (VEGF-B)	Prostaglandin-endoperoxide synthase 2 (COX2)	
Tumor Necrosis Factor-α (TNF-α)	Vascular Endothelial Growth Factor C (VEGF-C)	Tumor Necrosis Factor-α (TNF-α)	
Chemokine (CXC) ligand 1 (Gro1)	Vascular Endothelial Growth Factor (VEGF-D)	Chemokine (CXC) Ligand 1 (Gro1)	
Hepatocyte Growth Factor (HGF)	Fibroblast Growth Factor-1 (FGF1)	Hepatocyte Growth Factor (HGF)	
Platelet Endothelial Cell Adhesion Molecule (PECAM, CD31)	Interferon gamma (Ifng)	Platelet Endothelial Cell Adhesion Molecule (PECAM, CD31)	
Thrombospondin 1 (Thbs1)	Inhibitor of DNA Binding 3 (Idb, ID3)	Thrombospondin 1 (Thbs1)	
Transforming Growth Factor, beta receptor 2 (TGFbR2)	Connective Tissue Growth Factor (CTGF)	Transforming Growth Factor beta Receptor 2 (TGFbR2)	
Transforming Growth Factor, beta receptor 3 (TGFbR3)	Ephrin A2 (Efna2)	Transforming Growth Factor beta Receptor 3 (TGFbR3)	
Macrophage Scavenger Receptor 1 (Msr1)	Ephrin A5 (Efna5)	Macrophage Scavenger Receptor 1 (Msr1)	
Fibroblast Growth Factor Receptor 1 (FGFR1)	Ephrin B2 (Efnb2)	Vascular Endothelial Growth Factor A (VEGF-A)	
Serine Proteinase inhibitor, member 1 (PAI-1)	Epidermal Growth Factor (EGF)	Vascular Endothelial Growth Factor B (VEGF-B)	
Fibroblast Growth Factor Receptor 3 (FGFR3)	Eph Receptor B4 (Ephb4)	Vascular Endothelial Growth Factor C (VEGF-C)	
Colony Simulating Factor 3 (CSF3)	Fibroblast Growth Factor-4 (FGF4)	Vascular Endothelial Growth Factor D (VEGF-D)	
Interleukin 10 (IL10)	Interferon alpha family, gene 1 (Ifna1)	Connective Tissue Growth Factor (CTGF)	
Thrombospondin 2 (Thbs2)	Neuropilin (Nrp)	Fibroblast Growth Factor 1 (FGF1)	
A disintegrin metalloprotease thrombospondin type 1 motif (Adamts1)	Platelet Derived Growth Factor A (PDGFa)	Inhibitor of DNA Binding 3 (Idb3, ID3)	
	Platelet Derived Growth Factor B (PDGFb)	Interferon gamma (Ifng)	
	Placental Growth Factor (PGF)	Integrin alpha 5 (fibronectin receptor alpha) (Itga5)	
	Pleiotrophin (Ptn)	Integrin alpha V (ItgaV)	
	Chemokine (C-C) Ligand 2 (Ccl2)	Integrin beta 3 (Itgb3)	
	Serine proteinase inhibitor, member 5 (Maspin, Serpinb5)	Cadherin 5 (Cdh5, VE-cadherin)	
	Serine Proteinase inhibitor, member 2 (PAI-2, Serpinb2)	Vascular Cell Adhesion Molecule (VCAM)	
	Tyrosine Kinase Receptor 1 (Tie1)	Fibronectin 1 (Fn1)	
	Thrombospondin 4 (Thbs4)	Fibroblast Growth Factor 7 (FGF7)	
	Procollagen Type 18, alpha 1 (COL18A1) (Endostatin precursor)	Platelet Derived Growth Factor Receptor, alpha (PDGFRa)	
	Tissue Inhibitor of Metalloproteinase 2 (TIMP2)	Platelet Derived Growth Factor Receptor, beta (PDGFRb)	
	Transforming Growth Factor beta 3 (TGF-b3)	Insulin-like Growth Factor 1 (IGF1)	
		Plasminogen activator, Urokinase (PLAU)	
		Prostaglandin-endoperoxidase synthase 1 (PTGS1)	
		E26 Avian leukemia oncogene (Ets1)	
		MAD homolog 1 (Smad1)	
		Inhibitor of DNA Binding 1 (Idb1, ID1)	
		Secreted Phosphoprotein 1 (Osteopontin, Spp1)	
		Endothelial Specific Receptor Tyrosine Kinase (TEK, Tie2)	
		Erythroblastic leukemia viral oncogene homolog 2 (Neu/HER2, Erbb2)	
		Interleukin 12a (IL12a)	
		Secreted Acidic Cysteine Rich Glycoprotein (SPARC, BM-40)	
		Transforming Growth Factor beta 1 (TGFb1)	
		Transforming Growth Factor beta Receptor 1 (TGFbR1)	

Yellow background indicates genes up-regulated in both models. Blue background indicates genes down-regulated in both models.

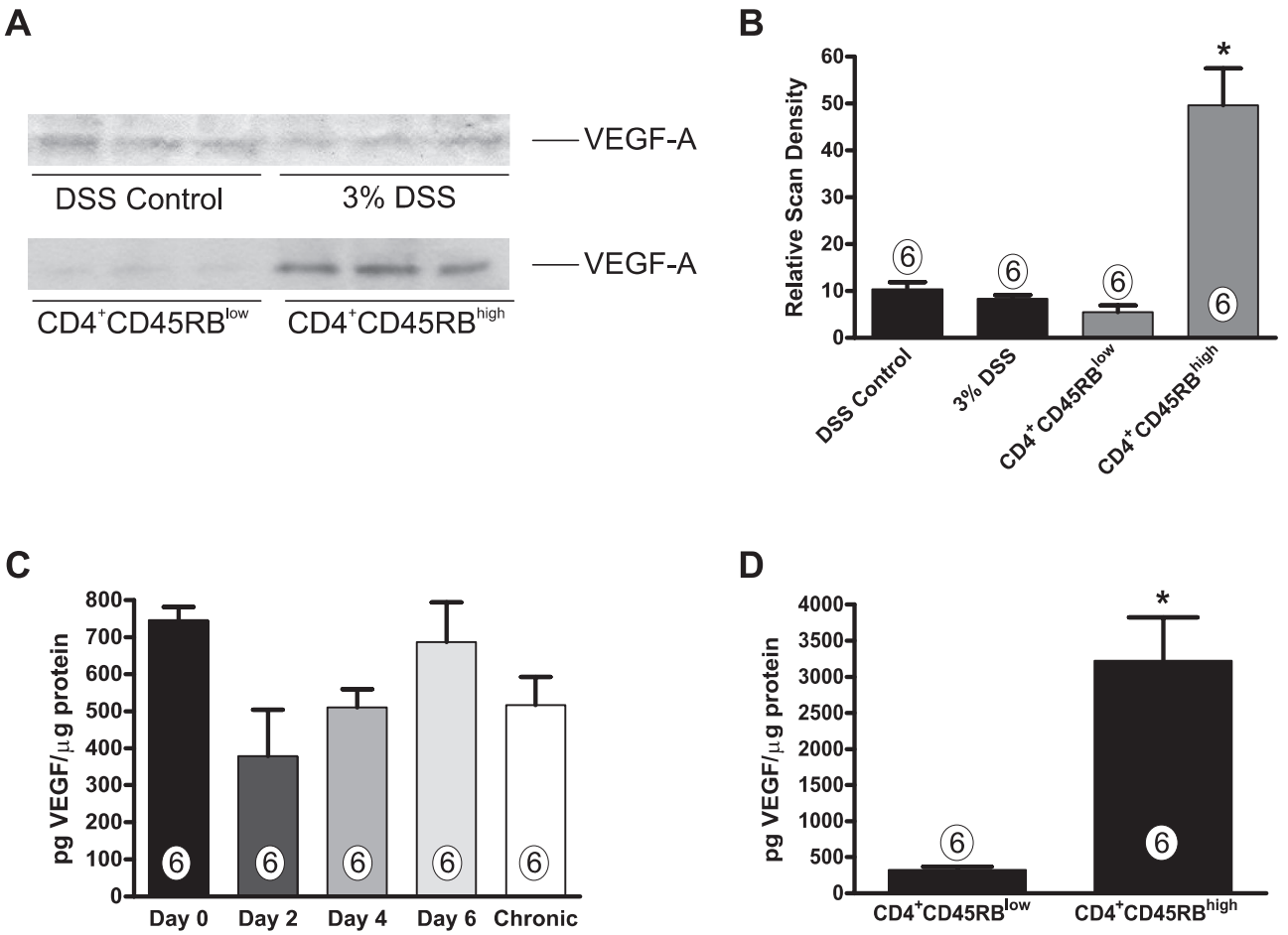

Figure 4. Measurement of VEGF-A expression levels during experimental colitis. VEGF-A protein levels were examined between the two experimental colitis models using Western blot and enzyme-linked immunodetection assays. Fifty μg of total protein tissue extract from control or experimental colitis colons was separated using SDS-polyacrylamide gel electrophoresis. **A:** VEGF-A protein levels by Western blot analysis between control and experimental colitis. **B:** Relative scan density of VEGF-A Western blots demonstrating a significant increase in VEGF-A protein in $CD4^+CD45RB^{high}$ colitis tissue extract. **C:** Temporal ELISA measurement of VEGF-A during DSS-induced colitis. **D:** ELISA measurement of VEGF-A protein (pg/μg total protein) in tissue extracts from $CD4^+CD45RB^{low}$ control and $CD4^+CD45RB^{high}$ T-cell transfer colons. *n* values for each experimental condition are reported within the bar graph. $^*P < 0.05$ versus control.

Differential regulation of numerous angiogenic mediators also occurred, revealing specific angiogenic differences between the two models. In the DSS model, several pro- and anti-angiogenic genes were up-regulated, but the same genes were unchanged in the $CD4^+CD45RB^{high}$ model. The proangiogenic factors include fibroblast growth factor receptors 1 and 3 (FGFR1, 3), serine protease inhibitor 1 (PAI-1), and colony stimulating factor 3 (CSF3). Those with anti-angiogenic effects are IL-10, thrombospondin 2 (Thbs2), and a disintegrin metalloproteinase thrombospondin type 1 motif (Adamts 1). However, many more anti-angiogenic genes (eg, Col18, TIMP-2, and so forth) were significantly down-regulated in DSS colitis, suggesting that angiogenic stimulation in this model is likely attributable to loss of negative regulators. Conversely, proangiogenic mediators were more substantially up-regulated in the $CD4^+CD45RB^{high}$ colitis model. Moreover, several molecules were distinctly up-regulated in $CD4^+CD45RB^{high}$ colitis yet down-regulated in DSS colitis, including connective tissue growth factor (CTGF), fibroblast growth factor-1 (FGF1), inhibitor of DNA binding 3 (ID3), and interferon-γ. Most interestingly, VEGF-A, -B, -C, and -D were all up-regulated in $CD4^+CD45RB^{high}$ colitis yet down-regulated in the DSS model, illustrating the unique nature of angiogenic gene expression between the two models. Together, these data suggest that neovascularization in the $CD4^+CD45RB^{high}$ model primarily involves up-regulation of proangiogenic factors, whereas neovascularization in the DSS model is associated with an abundant decrease in anti-angiogenic gene expression.

Differential expression of angiogenic factors, such as VEGF-A, have recently been reported in UC and CD.[9,11,12] Having observed distinct differences in VEGF-A gene expression between the two models, we examined VEGF-A protein levels present in serum and colon tissue from the DSS and $CD4^+CD45RB^{high}$ models by Western blot and ELISA. Western blots for VEGF-A did not reveal any significant difference in VEGF-A levels during DSS colitis (Figure 4A); however, densitometric analysis of the $CD4^+CD45RB^{high}$ VEGF-A Westerns showed a significant 9.5-fold increase in tissue VEGF levels (Figure 4B). VEGF-A ELISA was performed with tissue lysates to quantitate precisely the amount of VEGF-A produced. Having observed no change in VEGF-A protein levels on completion of the DSS model, we examined VEGF-A tissue levels at various

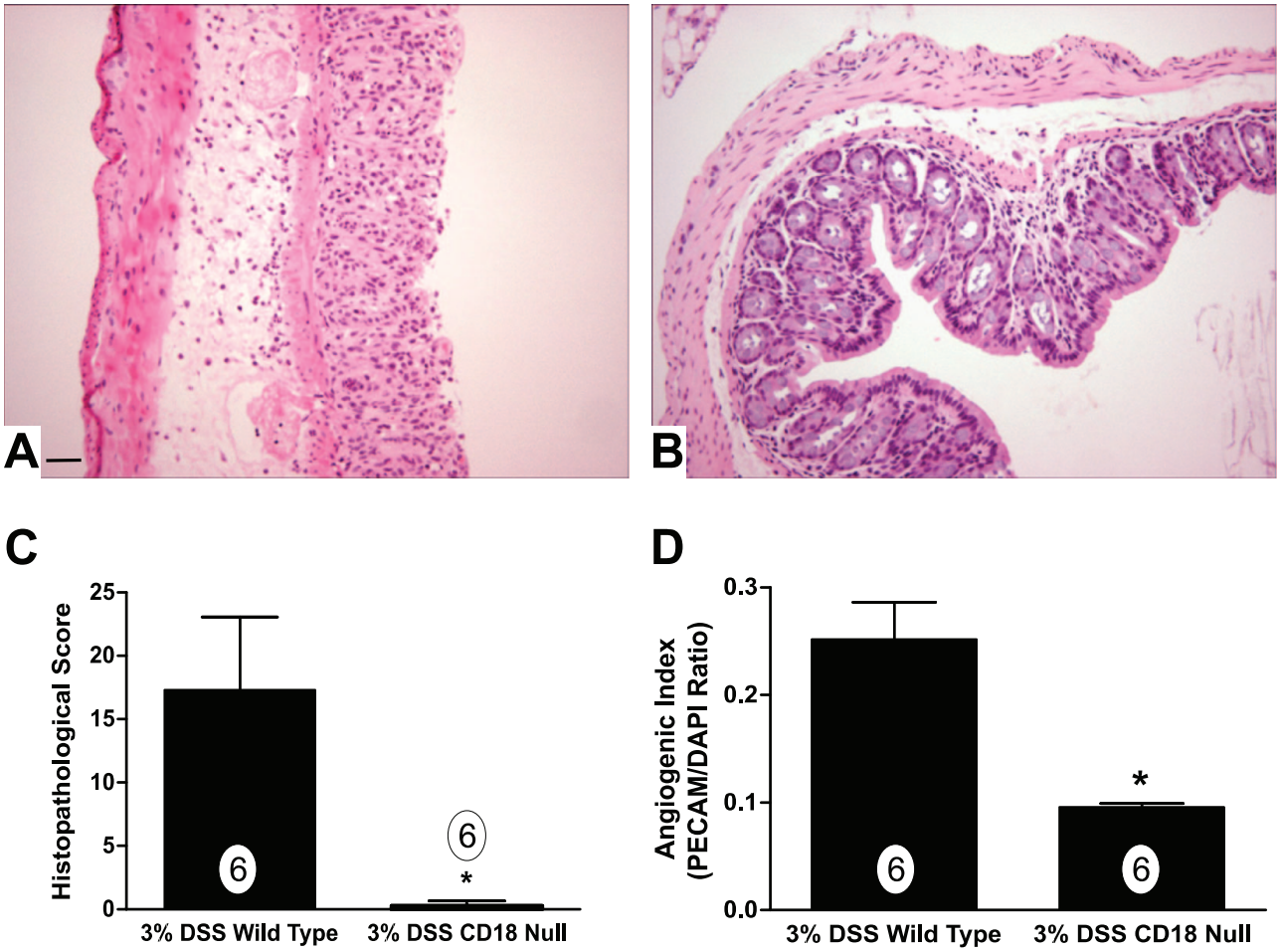

Figure 5. Leukocyte recruitment is required for angiogenic activity during experimental colitis. The importance of leukocyte recruitment for angiogenic stimulation during experimental colitis was examined using CD18-null mutant mice treated with 3% DSS. **A:** Illustrates 3% DSS histopathology of wild-type mice displaying prominent leukocyte infiltration, tissue edema, and epithelial cell damage. Conversely, **B** shows 3% DSS-mediated tissue pathology in CD18-null mutant mice. **C:** 3% DSS-mediated histopathological scores between wild-type and CD18-null mice. Likewise, **D** reports angiogenic index scores from 3% DSS-treated wild-type or CD18-null mice. *n* values for each condition are reported within the bar graph. Original magnifications, ×200. Scale bar = 100 μm. *$P < 0.05$ versus control.

time points in the DSS model to address the possibility of early changes in expression that could be lost because of tissue damage. Consistent with the angiogenesis gene array results, VEGF-A expression was not significantly different throughout DSS colitis. However, we observed a trend of decreased expression early during the colitis model that resolved by day 6 of the DSS model (Figure 4C). Thus, alteration of VEGF-A expression in the DSS model is not attributable to excessive tissue damage and/or protein loss. Moreover, VEGF-A expression was not increased on completion of the chronic DSS model. Conversely, a sevenfold increase in VEGF-A was observed in the colon tissue of $CD4^{+}CD45RB^{high}$ mice with a control concentration of 450 pg/μg of total protein versus 3300 pg/μg of total protein for colitic specimens (Figure 4D). Last, serum VEGF-A levels from both models did not reveal any significant differences between experimental and control groups (data not shown). Together, these data confirm results from the angiogenesis gene array experiments and provide clear evidence demonstrating different mechanisms of angiogenic stimulation between the two models.

Leukocyte Infiltration Governs Angiogenic Activity in Experimental Colitis

Infiltration of leukocytes into tissue has been shown to be associated with increased angiogenesis in various chronic inflammatory disorders and is believed to be an important mediator of pathological angiogenesis.[61–64] Therefore, we examined whether increased leukocyte infiltration is necessary for increased angiogenic activity observed during experimental colitis. The CD18-null mutant mouse, with its complete loss of leukocyte β_2 integrins, has a severely blunted ability to recruit leukocytes under inflammatory conditions and its loss attenuates chronic inflammatory disease.[65–67] We have recently shown that genetic ablation of CD18 confers protection against DSS colitis attributable to defective leukocyte infiltration.[30] Therefore, we determined the importance of leukocyte recruitment on angiogenic stimulation during experimental colitis using CD18-null mice treated with DSS. Histopathological analysis of wild-type mice re-

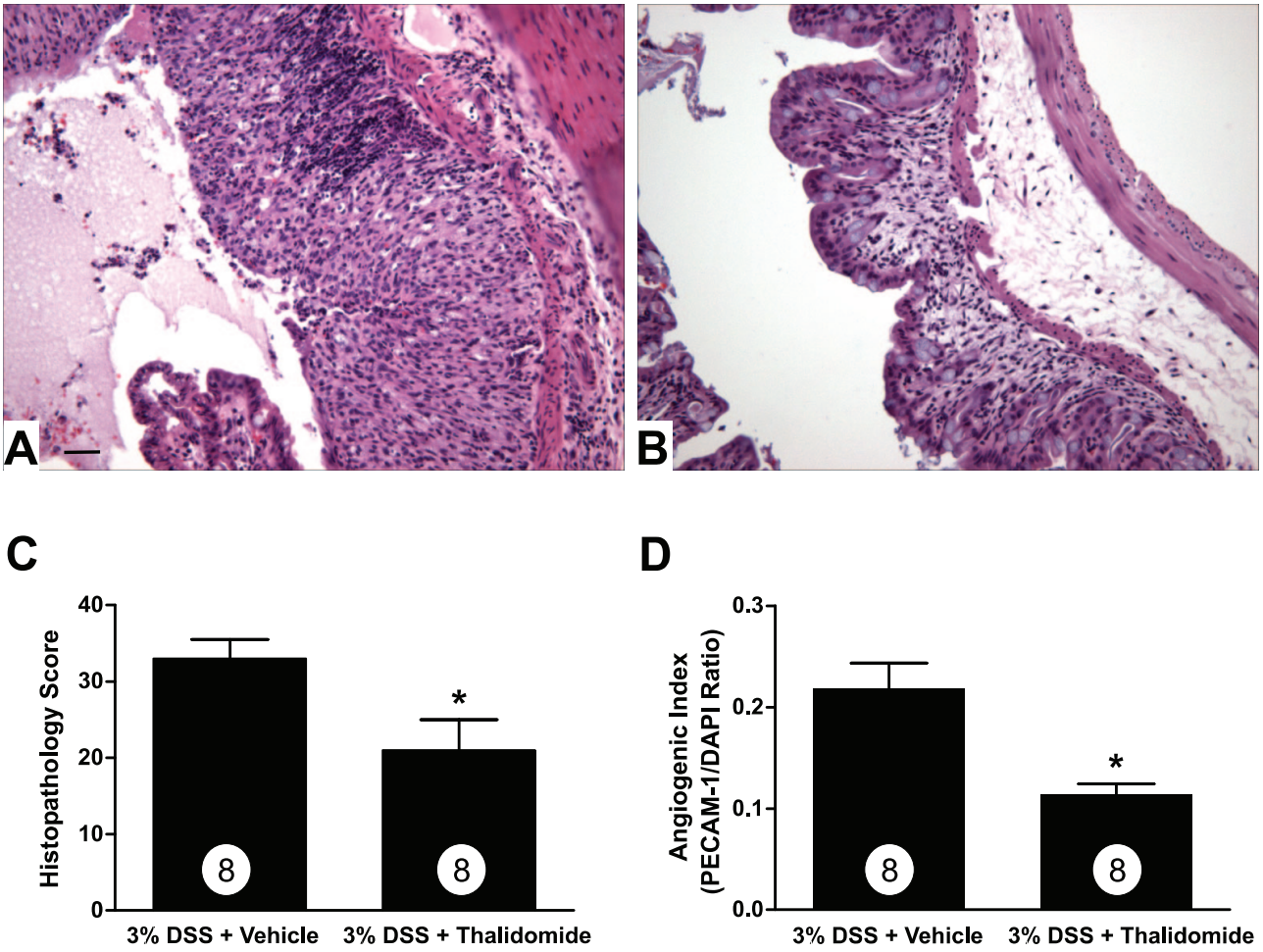

Figure 6. Thalidomide anti-angiogenic therapy attenuates DSS experimental colitis tissue pathology and neovascularization. The anti-angiogenic agent thalidomide (200 mg/kg) was used to evaluate the pathological importance of angiogenic activity during experimental colitis. **A:** Representative histomorphology from dimethyl sulfoxide vehicle-treated mice subjected to 3% DSS colitis. **B:** The effect of thalidomide treatment on 3% DSS-induced colitis. **C:** The tissue histopathology score between vehicle and thalidomide-treated mice subjected to 3% DSS colitis. Likewise, **D** demonstrates the angiogenic index between vehicle and thalidomide-treated mice subjected to 3% DSS colitis. *n* values for each condition are reported within the bar graph. $^*P < 0.05$ versus control. Original magnifications, ×200. Scale bar = 100 μm.

vealed a typical increase in leukocyte infiltrates in the mucosa and submucosa as well as extensive mucosal/crypt and epithelial cell layer damage, which was essentially absent in CD18-null colons treated with DSS (Figure 5, A and B, respectively). Histopathological scoring revealed an absence of DSS-mediated tissue damage as we have recently reported (Figure 5C).[30] Importantly, the angiogenic index of DSS CD18-null colons was found to be significantly reduced compared with DSS wild-type colons, 0.096 ± 0.003 versus 0.254 ± 0.034, respectively (Figure 5D). Together, these data demonstrate that leukocyte infiltration is an obligatory requirement for angiogenic stimulation during experimental colitis.

The Anti-Angiogenic Agent Thalidomide Attenuates Experimental Colitis

Data presented thus far demonstrate increased angiogenic activity during experimental colitis that is primarily dependent on inflammatory cells and mediators. However, no experimental evidence exists demonstrating that increased angiogenic activity plays a pathological role during colitis. Recent clinical reports suggest that the anti-angiogenic agent thalidomide is capable of inducing remission of active CD.[8] Given the unique nature of thalidomide as an anti-angiogenic and immunomodulatory agent, we determined whether thalidomide treatment affects DSS-induced colitis and neovascularization.[68,69] Figure 6, A and B, illustrates histopathological features of DSS plus dimethyl sulfoxide vehicle or DSS plus 200 mg/kg thalidomide, respectively. DSS-mediated histopathology showed that vehicle control mice develop significant tissue damage with perfuse immune cell infiltration associated with prominent mucosal/crypt and epithelial cell damage (Figure 6A). Conversely, thalidomide significantly blunted mucosal injury and leukocyte recruitment and preserved the mucosal epithelium compared with vehicle control colons (Figure 6B). DSS cumulative histopathology scores are shown in Figure 6C demonstrating a significant decrease in tissue damage in colons from thalidomide-treated mice. Moreover, the angiogenic index was also significantly decreased in thalidomide-treated mice compared with control mice (Figure 6D).

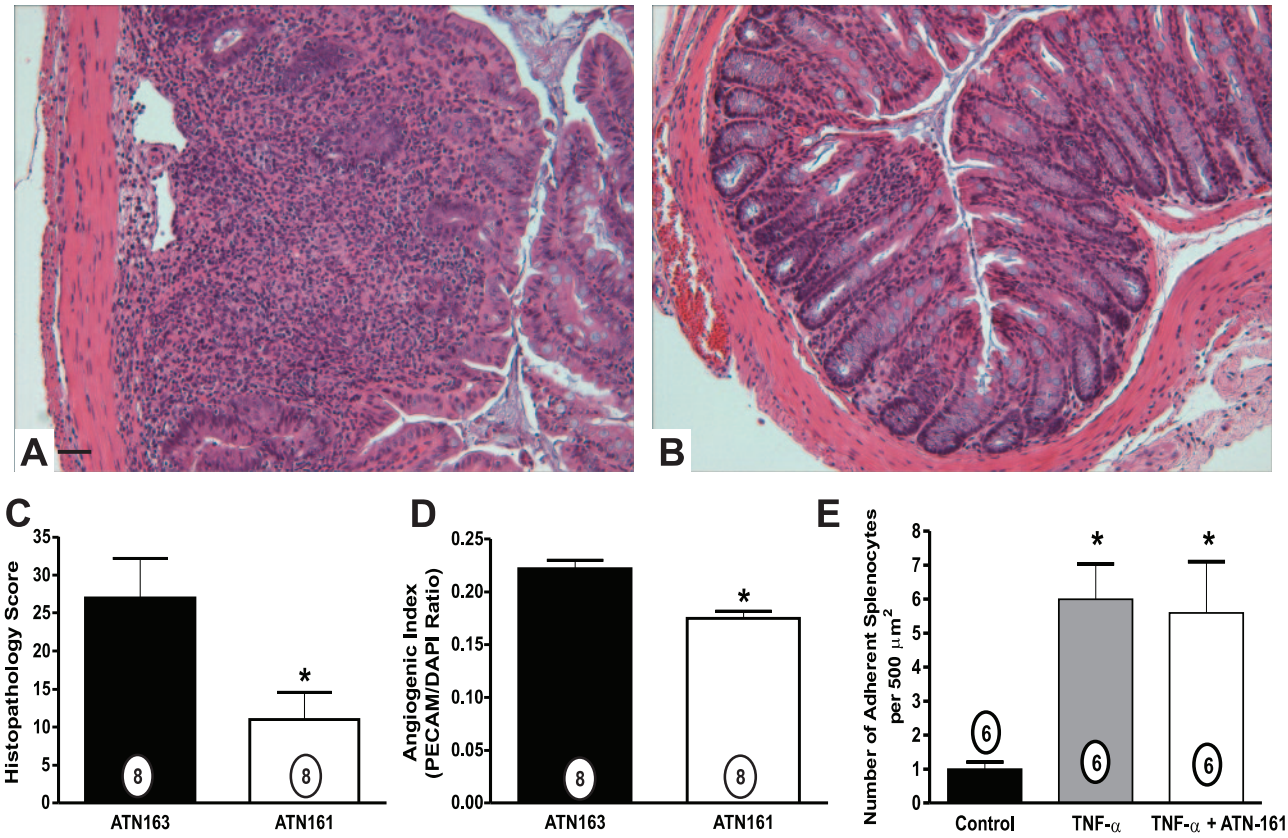

Figure 7. ATN-161 anti-angiogenic therapy attenuates $CD4^+CD45RB^{high}$ experimental colitis tissue damage and neovascularization. The $\alpha_5\beta_1$ and $\alpha_V\beta_3$ angiogenic integrin antagonist ATN-161 was used to determine the pathological importance of neovascularization during $CD4^+CD45RB^{high}$ colitis. **A:** Representative histopathology of mice treated with ATN-163 (1 mg/kg) control peptide. **B:** Representative histopathology of mice treated with active drug ATN-161 (1 mg/kg). Note the stark contrast in immune cell infiltrates and crypt architecture. **C:** The histopathology scores from mice treated with ATN-163 or ATN-161. **D:** The angiogenic index of mice treated with ATN-163 or ATN-161. **E:** The effect of 10 μg/ml ATN-161 on leukocyte adhesion to unstimulated and 10 ng/ml TNF-α-activated endothelial monolayers. *n* values for each group are reported within the bar graph. $^*P < 0.05$. Original magnifications, ×200. Scale bar = 100 μm.

These data demonstrate that angiogenic and inflammatory activity play key pathophysiological roles in the development of DSS-induced colitis.

Anti-Angiogenic Treatment of $CD4^+CD45RB^{high}$ Colitis Attenuates Disease

To substantiate that the therapeutic effects observed with thalidomide were attributable to the inhibition of angiogenesis, we used a selective anti-angiogenic peptide ATN-161 in the $CD4^+CD45RB^{high}$ colitis model. Angiogenesis gene array analysis of the $CD4^+CD45RB^{high}$ model revealed distinct up-regulation of α_5, α_V, and β_3 integrins and matrix ligands associated with neovascularization. The anti-angiogenic peptide ATN-161 attenuates neovascularization by binding $\alpha_5\beta_1$ and $\alpha_V\beta_3$ and has been reported to significantly attenuate tumor-mediated angiogenesis.[38] Figure 7 shows that 1 mg/kg ATN-163 (scrambled peptide) treatment did not alter histopathology of $CD4^+CD45RB^{high}$ colitis, whereas 1 mg/kg ATN-161 (active peptide) significantly decreased immune cell infiltration and edema and attenuated crypt destruction compared with ATN-163 control drug (Figure 7, A and B, respectively). Moreover, Figure 7, C and D, demonstrates that ATN161 significantly decreases both the tissue histopathology score and the angiogenic index, respectively. Studies have verified this compound as a potent and selective inhibitor of angiogenesis with no indication of a role in modulating inflammatory responses. ATN-161 was shown to be highly active in Matrigel plugs where angiogenesis is driven by VEGF or FGF-2, where the compound bound exclusively to neovessels.[38] In addition, ATN-161 selectively decreases viable EPCs, which are known to be involved in angiogenesis, while having no effect on CECs, which are associated with inflammation (A.P.M., personal communication). Nonetheless, given the possibility that ATN-161 might affect leukocyte function, we examined whether ATN-161 altered leukocyte recruitment and adhesion to activated endothelial monolayers. MS-1 mouse endothelial cells were stimulated with 10 ng/ml TNF-α and assembled in a parallel plate flow chamber system to evaluate mouse splenocyte adhesion under hydrodynamic flow conditions as we have previously reported.[39] Figure 7E clearly illustrates that 10 μg/ml ATN-161, the therapeutic dose used for *in vivo* experiments based on a total blood volume of 2.5 ml, did not alter TNF-α-mediated leukocyte adhesion. This finding corroborates the selectivity of ATN-161 and demonstrates that the agent does not interfere with inflammatory responses. Together, these

data using a select agent against angiogenic integrins demonstrate that increased neovascularization plays an important role in facilitating tissue damage and dysfunction during $CD4^+CD45RB^{high}$ colitis.

Discussion

Here we have shown that increased angiogenic activity in response to chronic inflammation plays an important pathophysiological role during experimental colitis. Several different models of experimental colitis have been reported to display similar pathophysiological findings of clinical CD or UC.[1,15,27,40] We used the DSS and the $CD4^+CD45RB^{high}$ T-cell transfer models of colitis because of the pathological similarities of UC and CD. Immunopathogenesis of the DSS model is mediated primarily by neutrophils and monocytes, resulting in extensive crypt and epithelial cell damage throughout a shorter experimental period.[15,70] Conversely, reconstitution of immunodeficient mice with an immunologically naive population of T cells termed $CD4^+CD45RB^{high}$ cells induces chronic pan-colitis 6 to 8 weeks after transfer, thus evoking a less severe protracted chronic inflammatory response.[16,71,72] Together, these models display several important pathophysiological features of human IBD, permitting detailed examination of angiogenic parameters during colitis that could facilitate angiogenesis during the development and progression of UC or CD.

Increased angiogenic activity has been observed in several chronic inflammatory diseases, yet the importance of this association and the manner in which angiogenesis is stimulated in IBD or experimental colitis remains unknown.[29,73,74] We found that blood vessel densities were significantly increased in both the DSS and $CD4^+CD45RB^{high}$ models of colitis. Moreover, the majority of the vasculature was perfused as determined by intravascular FITC-lectin binding to endothelium.[54] A strong correlation between the overall angiogenic index and histopathological score was also found in tissue sections from both models. In addition, the increase in neovascularization temporally coincided with increased tissue histopathology. Together, these data strongly suggest that stimulation of angiogenic activity is an active participant in the pathological process of experimental colitis.

Stimulation of angiogenesis is complex and dynamic with different mediators influencing neovascularization in a tissue- and disease-specific manner.[56,75] It is increasingly accepted that angiogenic activity occurs in both physiological and pathological settings resulting in clear differences in vascular phenotypes.[56] As such, differential regulation of the angiogenic response is influenced by the type of mediator, either positive or negative, and the degree of its expression, either up or down.[76–78] Here we show that there are a small group of angiogenic mediators that are similarly controlled between the two models of experimental colitis. However, we also found differential regulation of numerous angiogenic genes between the two models, with the majority being down-regulated in DSS colitis and up-regulated in $CD4^+CD45RB^{high}$ colitis. Importantly, several potent anti-angiogenic or angiostatic genes were significantly down-regulated in the DSS model, including CD36, chromogranin A, thrombospondin 4, collagen type 18 (endostatin precursor), and TIMP-2 versus the $CD4^+CD45RB^{high}$ model that only included CD36 and chromogranin A. These data suggest that angiogenesis may primarily occur in the DSS model through loss of angiogenic inhibition. Conversely, angiogenesis in the $CD4^+CD45RB^{high}$ model likely occurs because of dramatic differential up-regulation of proangiogenic mediators (34 genes) compared with anti-angiogenic mediators (three genes). Several explanations could account for the difference in angiogenic gene expression between the two models, with the manner of colitis induction and the type of immune cell involved being obvious possibilities. Together, our findings suggest that interventions aimed at increasing and restoring anti-angiogenic activity versus blockade of proangiogenic mediators may provide additional selective means for treating various forms of IBD.

Protein expression analysis of VEGF-A between the two models confirmed the differential gene array data reinforcing the notion that angiogenic stimulation in the two models is clearly different. VEGF-A is widely regarded as a classic angiogenic cytokine because of its plethoric role in stimulating various endothelial cell responses necessary for angiogenesis.[79–84] Moreover, VEGF-A has been reported to be important for both physiological and pathological angiogenesis, indicating that this molecule may be central for multiple angiogenic responses.[85] We were surprised to find that VEGF-A expression was significantly enhanced in the $CD4^+CD45RB^{high}$ T-cell transfer model but not in the DSS model. However, a recent study by Konno and colleagues[12] has reported differential VEGF expression in UC versus CD tissue, corroborating our findings. These data reinforce the idea that targeted anti-angiogenic therapy in IBD may be most useful in treating specific classifications of colitis. Additional clinical and experimental investigation is required to better understand such differences and whether they may be exploited for intervention.

Palliative treatment of IBD has historically been accomplished through the use of aminosalicylates, steroids, or antibiotics along with the more recent use of immunomodulators including azathioprine, mercaptopurine, methotrexate, cyclosporine, and TNF-α blockade (Remicade). Unfortunately, all of these interventions may be limited in their efficacy and are associated with substantial side effects.[5,86,87] Thus, there have been minimal advances in the ability to prevent or cure IBD. Therefore, we examined the effect of anti-angiogenic intervention on experimental colitis. Thalidomide is an anti-angiogenic and immunomodulatory agent that has successfully induced remission of active IBD, but its ability to attenuate experimental colitis and its associated angiogenic activity is not known.[8,88,89] The molecular effects of thalidomide are many and include increased endothelial ceramide production that could facilitate apoptosis, decreased endothelial cell Akt activation that diminishes cell motility, differential gene regulation of endothelial cell growth factors and their receptors, and attenuation of

TNF-α and leukocyte responses, all of which are likely to be involved in the angiogenic response during experimental colitis.[68,69,90–92] Thalidomide treatment in the DSS model significantly attenuated disease as observed by a dramatic decrease in pathology score and angiogenic index compared with vehicle control mice. Given the biological mechanisms of thalidomide, these findings further demonstrate an important link between angiogenesis and inflammation during experimental colitis.

We also showed that selective anti-angiogenic inhibition of $\alpha_5\beta_1$ and $\alpha_V\beta_3$, which were selectively up-regulated in the $CD4^+CD45RB^{high}$ model, by ATN-161 significantly attenuated experimental colitis, providing evidence that targeting the neovasculature alone clearly protects against tissue damage. Thus, our results provide strong evidence for a pathological angiogenesis paradigm and that therapeutic targeting of angiogenesis may be clinically useful for IBD. However, future studies directly targeting additional angiogenic factors are needed to understand better the key mediators of angiogenesis during experimental colitis.

In summary, these data demonstrate that experimental colitis is characterized by angiogenic inflammation that contributes to the development and sustenance of experimental colitis. Our data provide a compelling argument that increased leukocyte recruitment is required for angiogenic stimulation during colitis. The ability to decrease angiogenic activity by preventing the inflammatory response with the CD18-null mouse model further solidifies the link between the two. Moreover, the angiogenic responses seen in experimental colitis may contribute to chronic inflammation, which likely enables a vicious cycle of disease activity. Indeed, we have recently reported that high concentrations of angiogenic cytokines, such as VEGF-A, increase leukocyte interactions with colon microvascular endothelial cells similar to proinflammatory agents such as TNF-α.[39] The ability of the anti-angiogenic agents thalidomide and ATN-161 to significantly attenuate experimental colitis demonstrates that anti-angiogenic therapies could provide novel treatments for IBD.

Acknowledgments

We thank Dr. Neil Granger and Ms. Janice Russell for assistance with dual radiolabel antibody detection of PECAM-1, and Mr. Lamar Jones for expert technical assistance.

References

1. Elson CO, Sartor RB, Tennyson GS, Riddell RH: Experimental models of inflammatory bowel disease. Gastroenterology 1995, 109:1344–1367
2. Laroux FS, Grisham MB: Immunological basis of inflammatory bowel disease: role of the microcirculation. Microcirculation 2001, 8:283–301
3. Sartor RB: Pathogenesis and immune mechanisms of chronic inflammatory bowel diseases. Am J Gastroenterol 1997, 92:5S–11S
4. Wen Z, Fiocchi C: Inflammatory bowel disease: autoimmune or immune-mediated pathogenesis? Clin Dev Immunol 2004, 11:195–204
5. Ardizzone S, Porro GB: Inflammatory bowel disease: new insights into pathogenesis and treatment. J Intern Med 2002, 252:475–496
6. Spalinger J, Patriquin H, Miron MC, Marx G, Herzog D, Dubois J, Dubinsky M, Seidman EG: Doppler US in patients with Crohn disease: vessel density in the diseased bowel reflects disease activity. Radiology 2000, 217:787–791
7. Maconi G, Sampietro GM, Russo A, Bollani S, Cristaldi M, Parente F, Dottorini F, Bianchi Porro G: The vascularity of internal fistulae in Crohn's disease: an in vivo power Doppler ultrasonography assessment. Gut 2002, 50:496–500
8. Fishman SJ, Feins NR, D'Amato RJ, Folkman J: Long-term remission of Crohn's disease treated with thalidomide: a seminal case report. Angiogenesis 1999, 3:201–204
9. Bousvaros A, Leichtner A, Zurakowski D, Kwon J, Law T, Keough K, Fishman S: Elevated serum vascular endothelial growth factor in children and young adults with Crohn's disease. Dig Dis Sci 1999, 44:424–430
10. Kanazawa S, Tsunoda T, Onuma E, Majima T, Kagiyama M, Kikuchi K: VEGF, basic-FGF, and TGF-beta in Crohn's disease and ulcerative colitis: a novel mechanism of chronic intestinal inflammation. Am J Gastroenterol 2001, 96:822–828
11. Kapsoritakis A, Sfiridaki A, Maltezos E, Simopoulos K, Giatromanolaki A, Sivridis E, Koukourakis MI: Vascular endothelial growth factor in inflammatory bowel disease. Int J Colorectal Dis 2003, 18:418–422
12. Konno S, Iizuka M, Yukawa M, Sasaki K, Sato A, Horie Y, Nanjo H, Fukushima T, Watanabe S: Altered expression of angiogenic factors in the VEGF-Ets-1 cascades in inflammatory bowel disease. J Gastroenterol 2004, 39:931–939
13. Ozawa CR, Banfi A, Glazer NL, Thurston G, Springer ML, Kraft PE, McDonald DM, Blau HM: Microenvironmental VEGF concentration, not total dose, determines a threshold between normal and aberrant angiogenesis. J Clin Invest 2004, 113:516–527
14. Bousvaros A, Zurakowski D, Fishman SJ, Keough K, Law T, Sun C, Leichtner AM: Serum basic fibroblast growth factor in pediatric Crohn's disease. Implications for wound healing. Dig Dis Sci 1997, 42:378–386
15. Pizarro TT, Arseneau KO, Bamias G, Cominelli F: Mouse models for the study of Crohn's disease. Trends Mol Med 2003, 9:218–222
16. Laroux FS, Norris HH, Houghton J, Pavlick KP, Bharwani S, Merrill DM, Fuseler J, Chervenak R, Grisham MB: Regulation of chronic colitis in athymic nu/nu (nude) mice. Int Immunol 2004, 16:77–89
17. Abreu MT: The pathogenesis of inflammatory bowel disease: translational implications for clinicians. Curr Gastroenterol Rep 2002, 4:481–489
18. Toms C, Powrie F: Control of intestinal inflammation by regulatory T cells. Microbes Infect 2001, 3:929–935
19. Shamamian P, Schwartz JD, Pocock BJ, Monea S, Whiting D, Marcus SG, Mignatti P: Activation of progelatinase A (MMP-2) by neutrophil elastase, cathepsin G, and proteinase-3: a role for inflammatory cells in tumor invasion and angiogenesis. J Cell Physiol 2001, 189:197–206
20. Kasama T, Kobayashi K, Yajima N, Shiozawa F, Yoda Y, Takeuchi HT, Mori Y, Negishi M, Ide H, Adachi M: Expression of vascular endothelial growth factor by synovial fluid neutrophils in rheumatoid arthritis (RA). Clin Exp Immunol 2000, 121:533–538
21. Cassatella MA: Neutrophil-derived proteins: selling cytokines by the pound. Adv Immunol 1999, 73:369–509
22. Schruefer R, Lutze N, Schymeinsky J, Walzog B: Human neutrophils promote angiogenesis by a paracrine feedforward mechanism involving endothelial interleukin-8. Am J Physiol 2005, 288:H1186–H1192
23. Kusumanto YH, Dam WA, Hospers GA, Meijer C, Mulder NH: Platelets and granulocytes, in particular the neutrophils, form important compartments for circulating vascular endothelial growth factor. Angiogenesis 2003, 6:283–287
24. Polverini PJ: Role of the macrophage in angiogenesis-dependent diseases. EXS 1997, 79:11–28
25. Sunderkötter C, Steinbrink K, Goebeler M, Bhardwaj R, Sorg C: Macrophages and angiogenesis. J Leukoc Biol 1994, 55:410–422
26. Knowles H, Leek R, Harris AL: Macrophage infiltration and angiogenesis in human malignancy. Novartis Found Symp 2004, 256:189–200, discussion 184–200, 169–259
27. Powrie F: Immune regulation in the intestine: a balancing act between effector and regulatory T cell responses. Ann NY Acad Sci 2004, 1029:132–141
28. Ten Hove T, The Olle F, Berkhout M, Bruggeman JP, Vyth-Dreese FA,

Slors JF, Van Deventer SJ, Te Velde AA: Expression of CD45RB functionally distinguishes intestinal T lymphocytes in inflammatory bowel disease. J Leukoc Biol 2004, 75:1010–1015
29. Naldini A, Carraro F: Role of inflammatory mediators in angiogenesis. Curr Drug Targets Inflamm Allergy 2005, 4:3–8
30. Abdelbaqi M, Chidlow JH, Matthews KM, Pavlick KP, Barlow SC, Linscott AJ, Grisham MB, Fowler MR, Kevil CG: Regulation of dextran sodium sulfate induced colitis by leukocyte beta 2 integrins. Lab Invest 2006, 86:380–390
31. Murthy S, Cooper HS, Yoshitake H, Meyer C, Meyer CJ, Murthy NS: Combination therapy of pentoxifylline and TNFalpha monoclonal antibody in dextran sulphate-induced mouse colitis. Aliment Pharmacol Ther 1999, 13:251–260
32. Pavlick KP, Ostanin DV, Furr KL, Laroux FS, Brown CM, Gray L, Kevil CG, Grisham MB: Role of T-cell-associated lymphocyte function-associated antigen-1 in the pathogenesis of experimental colitis. Int Immunol 2006, 18:389–398
33. Langley RR, Russell J, Eppihimer MJ, Alexander SJ, Gerritsen M, Specian RD, Granger DN: Quantification of murine endothelial cell adhesion molecules in solid tumors. Am J Physiol 1999, 277:H1156–H1166
34. Hashizume H, Baluk P, Morikawa S, McLean JW, Thurston G, Roberge S, Jain RK, McDonald DM: Openings between defective endothelial cells explain tumor vessel leakiness. Am J Pathol 2000, 156:1363–1380
35. Kevil CG, Walsh L, Laroux FS, Kalogeris T, Grisham MB, Alexander JS: An improved, rapid Northern protocol. Biochem Biophys Res Commun 1997, 238:277–279
36. Kevil CG, De Benedetti A, Payne DK, Coe LL, Laroux FS, Alexander JS: Translational regulation of vascular permeability factor by eukaryotic initiation factor 4E: implications for tumor angiogenesis. Int J Cancer 1996, 65:785–790
37. Kevil CG, Orr AW, Langston W, Mickett K, Murphy-Ullrich J, Patel RP, Kucik DF, Bullard DC: Intercellular adhesion molecule-1 (ICAM-1) regulates endothelial cell motility through a nitric oxide-dependent pathway. J Biol Chem 2004, 279:19230–19238
38. Stoeltzing O, Liu W, Reinmuth N, Fan F, Parry GC, Parikh AA, McCarty MF, Bucana CD, Mazar AP, Ellis LM: Inhibition of integrin alpha5beta1 function with a small peptide (ATN-161) plus continuous 5-FU infusion reduces colorectal liver metastases and improves survival in mice. Int J Cancer 2003, 104:496–503
39. Goebel S, Huang M, Davis WC, Jennings M, Siahaan TJ, Alexander JS, Kevil CG: VEGF-A stimulation of leukocyte adhesion to colonic microvascular endothelium: implications for inflammatory bowel disease. Am J Physiol 2006, 290:G648–G654
40. Powrie F, Uhlig H: Animal models of intestinal inflammation: clues to the pathogenesis of inflammatory bowel disease. Novartis Found Symp 2004, 263:164–211
41. Okayasu I, Hatakeyama S, Yamada M, Ohkusa T, Inagaki Y, Nakaya R: A novel method in the induction of reliable experimental acute and chronic ulcerative colitis in mice. Gastroenterology 1990, 98:694–702
42. Dieleman LA, Ridwan BU, Tennyson GS, Beagley KW, Bucy RP, Elson CO: Dextran sulfate sodium-induced colitis occurs in severe combined immunodeficient mice. Gastroenterology 1994, 107:1643–1652
43. Asseman C, Mauze S, Leach MW, Coffman RL, Powrie F: An essential role for interleukin 10 in the function of regulatory T cells that inhibit intestinal inflammation. J Exp Med 1999, 190:995–1004
44. Singh B, Read S, Asseman C, Malmstrom V, Mottet C, Stephens LA, Stepankova R, Tlaskalova H, Powrie F: Control of intestinal inflammation by regulatory T cells. Immunol Rev 2001, 182:190–200
45. Berger R, Albelda SM, Berd D, Ioffreda M, Whitaker D, Murphy GF: Expression of platelet-endothelial cell adhesion molecule-1 (PECAM-1) during melanoma-induced angiogenesis in vivo. J Cutan Pathol 1993, 20:399–406
46. DeLisser HM, Christofidou-Solomidou M, Strieter RM, Burdick MD, Robinson CS, Wexler RS, Kerr JS, Garlanda C, Merwin JR, Madri JA, Albelda SM: Involvement of endothelial PECAM-1/CD31 in angiogenesis. Am J Pathol 1997, 151:671–677
47. Sharma S, Sharma MC, Sarkar C: Morphology of angiogenesis in human cancer: a conceptual overview, histoprognostic perspective and significance of neoangiogenesis. Histopathology 2005, 46:481–489
48. Leek RD: The prognostic role of angiogenesis in breast cancer. Anticancer Res 2001, 21:4325–4331
49. Connor EM, Eppihimer MJ, Morise Z, Granger DN, Grisham MB: Expression of mucosal addressin cell adhesion molecule-1 (MAdCAM-1) in acute and chronic inflammation. J Leukoc Biol 1999, 65:349–355
50. Cid MC, Cebrian M, Font C, Coll-Vinent B, Hernandez-Rodriguez J, Esparza J, Urbano-Marquez A, Grau JM: Cell adhesion molecules in the development of inflammatory infiltrates in giant cell arteritis: inflammation-induced angiogenesis as the preferential site of leukocyte-endothelial cell interactions. Arthritis Rheum 2000, 43:184–194
51. Christofidou-Solomidou M, Nakada MT, Williams J, Muller WA, DeLisser HM: Neutrophil platelet endothelial cell adhesion molecule-1 participates in neutrophil recruitment at inflammatory sites and is down-regulated after leukocyte extravasation. J Immunol 1997, 158:4872–4878
52. Eppihimer MJ, Russell J, Langley R, Vallien G, Anderson DC, Granger DN: Differential expression of platelet-endothelial cell adhesion molecule-1 (PECAM-1) in murine tissues. Microcirculation 1998, 5:179–188
53. Müller AM, Hermanns MI, Skrzynski C, Nesslinger M, Muller KM, Kirkpatrick CJ: Expression of the endothelial markers PECAM-1, vWf, and CD34 in vivo and in vitro. Exp Mol Pathol 2002, 72:221–229
54. Ezaki T, Baluk P, Thurston G, La Barbara A, Woo C, McDonald DM: Time course of endothelial cell proliferation and microvascular remodeling in chronic inflammation. Am J Pathol 2001, 158:2043–2055
55. Jackson JR, Seed MP, Kircher CH, Willoughby DA, Winkler JD: The codependence of angiogenesis and chronic inflammation. FASEB J 1997, 11:457–465
56. Carmeliet P, Jain RK: Angiogenesis in cancer and other diseases. Nature 2000, 407:249–257
57. Creamer D, Sullivan D, Bicknell R, Barker J: Angiogenesis in psoriasis. Angiogenesis 2002, 5:231–236
58. Moulton KS, Heller E, Konerding MA, Flynn E, Palinski W, Folkman J: Angiogenesis inhibitors endostatin or TNP-470 reduce intimal neovascularization and plaque growth in apolipoprotein E-deficient mice. Circulation 1999, 99:1726–1732
59. Moulton KS, Vakili K, Zurakowski D, Soliman M, Butterfield C, Sylvin E, Lo KM, Gillies S, Javaherian K, Folkman J: Inhibition of plaque neovascularization reduces macrophage accumulation and progression of advanced atherosclerosis. Proc Natl Acad Sci USA 2003, 100:4736–4741
60. Griggs J, Skepper JN, Smith GA, Brindle KM, Metcalfe JC, Hesketh R: Inhibition of proliferative retinopathy by the anti-vascular agent combretastatin-A4. Am J Pathol 2002, 160:1097–1103
61. Croll SD, Ransohoff RM, Cai N, Zhang Q, Martin FJ, Wei T, Kasselman LJ, Kintner J, Murphy AJ, Yancopoulos GD, Wiegand SJ: VEGF-mediated inflammation precedes angiogenesis in adult brain. Exp Neurol 2004, 187:388–402
62. Ishida S, Yamashiro K, Usui T, Kaji Y, Ogura Y, Hida T, Honda Y, Oguchi Y, Adamis AP: Leukocytes mediate retinal vascular remodeling during development and vaso-obliteration in disease. Nat Med 2003, 9:781–788
63. Joussen AM, Poulaki V, Le ML, Koizumi K, Esser C, Janicki H, Schraermeyer U, Kociok N, Fauser S, Kirchhof B, Kern TS, Adamis AP: A central role for inflammation in the pathogenesis of diabetic retinopathy. FASEB J 2004, 18:1450–1452
64. Yasuda M, Shimizu S, Ohhinata K, Naito S, Tokuyama S, Mori Y, Kiuchi Y, Yamamoto T: Differential roles of ICAM-1 and E-selectin in polymorphonuclear leukocyte-induced angiogenesis. Am J Physiol 2002, 282:C917–C925
65. Scharffetter-Kochanek K, Lu H, Norman K, van Nood N, Munoz F, Grabbe S, McArthur M, Lorenzo I, Kaplan S, Ley K, Smith CW, Montgomery CA, Rich S, Beaudet AL: Spontaneous skin ulceration and defective T cell function in CD18 null mice. J Exp Med 1998, 188:119–131
66. Kevil CG, Hicks MJ, He X, Zhang J, Ballantyne CM, Raman C, Schoeb TR, Bullard DC: Loss of LFA-1, but not Mac-1, protects MRL/MpJ-Fas(lpr) mice from autoimmune disease. Am J Pathol 2004, 165:609–616
67. Barlow SC, Langston W, Matthews KM, Chidlow Jr JH, Kevil CG: CD18 deficiency protects against multiple low-dose streptozotocin-induced diabetes. Am J Pathol 2004, 165:1849–1852
68. D'Amato RJ, Loughnan MS, Flynn E, Folkman J: Thalidomide is an

inhibitor of angiogenesis. Proc Natl Acad Sci USA 1994, 91:4082–4085
69. Sampaio EP, Sarno EN, Galilly R, Cohn ZA, Kaplan G: Thalidomide selectively inhibits tumor necrosis factor alpha production by stimulated human monocytes. J Exp Med 1991, 173:699–703
70. Krieglstein CF, Cerwinka WH, Sprague AG, Laroux FS, Grisham MB, Koteliansky VE, Senninger N, Granger DN, de Fougerolles AR: Collagen-binding integrin alpha1beta1 regulates intestinal inflammation in experimental colitis. J Clin Invest 2002, 110:1773–1782
71. Powrie F, Leach MW, Mauze S, Caddle LB, Coffman RL: Phenotypically distinct subsets of CD4+ T cells induce or protect from chronic intestinal inflammation in C. B-17 scid mice. Int Immunol 1993, 5:1461–1471
72. Morrissey PJ, Charrier K: Induction of wasting disease in SCID mice by the transfer of normal CD4+/CD45RBhi T cells and the regulation of this autoreactivity by CD4+/CD45RBlo T cells. Res Immunol 1994, 145:357–362
73. Majno G: Chronic inflammation: links with angiogenesis and wound healing. Am J Pathol 1998, 153:1035–1039
74. Mor F, Quintana FJ, Cohen IR: Angiogenesis-inflammation cross-talk: vascular endothelial growth factor is secreted by activated T cells and induces Th1 polarization. J Immunol 2004, 172:4618–4623
75. Carmeliet P, Collen D: Molecular analysis of blood vessel formation and disease. Am J Physiol 1997, 273:H2091–H2104
76. Kahn J, Mehraban F, Ingle G, Xin X, Bryant JE, Vehar G, Schoenfeld J, Grimaldi CJ, Peale F, Draksharapu A, Lewin DA, Gerritsen ME: Gene expression profiling in an in vitro model of angiogenesis. Am J Pathol 2000, 156:1887–1900
77. Peale Jr FV, Gerritsen ME: Gene profiling techniques and their application in angiogenesis and vascular development. J Pathol 2001, 195:7–19
78. Gerritsen ME, Peale Jr FV, Wu T: Gene expression profiling in silico: relative expression of candidate angiogenesis associated genes in renal cell carcinomas. Exp Nephrol 2002, 10:114–119
79. Kevil CG, Payne DK, Mire E, Alexander JS: Vascular permeability factor/vascular endothelial cell growth factor-mediated permeability occurs through disorganization of endothelial junctional proteins. J Biol Chem 1998, 273:15099–15103
80. Morbidelli L, Chang CH, Douglas JG, Granger HJ, Ledda F, Ziche M: Nitric oxide mediates mitogenic effect of VEGF on coronary venular endothelium. Am J Physiol 1996, 270:H411–H415
81. Papapetropoulos A, Garcia-Cardena G, Madri JA, Sessa WC: Nitric oxide production contributes to the angiogenic properties of vascular endothelial growth factor in human endothelial cells. J Clin Invest 1997, 100:3131–3139
82. Kroll J, Waltenberger J: The vascular endothelial growth factor receptor KDR activates multiple signal transduction pathways in porcine aortic endothelial cells. J Biol Chem 1997, 272:32521–32527
83. Gerber HP, McMurtrey A, Kowalski J, Yan M, Keyt BA, Dixit V, Ferrara N: Vascular endothelial growth factor regulates endothelial cell survival through the phosphatidylinositol 3′-kinase/Akt signal transduction pathway. Requirement for Flk-1/KDR activation. J Biol Chem 1998, 273:30336–30343
84. Pedram A, Razandi M, Levin ER: Extracellular signal-regulated protein kinase/Jun kinase cross-talk underlies vascular endothelial cell growth factor-induced endothelial cell proliferation. J Biol Chem 1998, 273:26722–26728
85. Ferrara N: The role of VEGF in the regulation of physiological and pathological angiogenesis. EXS 2005, (94)209–231
86. Farthing MJ: Severe inflammatory bowel disease: medical management. Dig Dis 2003, 21:46–53
87. Kusugami K, Ina K, Ando T, Hibi K, Nishio Y, Goto H: Immunomodulatory therapy for inflammatory bowel disease. J Gastroenterol 2004, 39:1129–1137
88. Bauditz J, Wedel S, Lochs H: Thalidomide reduces tumour necrosis factor alpha and interleukin 12 production in patients with chronic active Crohn's disease. Gut 2002, 50:196–200
89. Bariol C, Meagher AP, Vickers CR, Byrnes DJ, Edwards PD, Hing M, Wettstein AR, Field A: Early studies on the safety and efficacy of thalidomide for symptomatic inflammatory bowel disease. J Gastroenterol Hepatol 2002, 17:135–139
90. Dredge K, Horsfall R, Robinson SP, Zhang LH, Lu L, Tang Y, Shirley MA, Muller G, Schafer P, Stirling D, Dalgleish AG, Bartlett JB: Orally administered lenalidomide (CC-5013) is anti-angiogenic in vivo and inhibits endothelial cell migration and Akt phosphorylation in vitro. Microvasc Res 2005, 69:56–63
91. Yabu T, Tomimoto H, Taguchi Y, Yamaoka S, Igarashi Y, Okazaki T: Thalidomide-induced anti-angiogenic action is mediated by ceramide through depletion of VEGF receptors, and antagonized by sphingosine-1-phosphate. Blood 2005, 106:125–134
92. Liu J, Razani B, Tang S, Terman BI, Ware JA, Lisanti MP: Angiogenesis activators and inhibitors differentially regulate caveolin-1 expression and caveolae formation in vascular endothelial cells. Angiogenesis inhibitors block vascular endothelial growth factor-induced down-regulation of caveolin-1. J Biol Chem 1999, 274:15781–15785